#### ORIGINAL PAPER



# A toric deformation method for solving Kuramoto equations on cycle networks

Tianran Chen · Robert Davis

Received: 26 November 2020 / Accepted: 14 May 2022 © The Author(s), under exclusive licence to Springer Nature B.V. 2022

**Abstract** The study of frequency synchronization configurations in Kuramoto models for networks of coupled oscillators is a ubiquitous mathematical problem that has found applications in many seemingly independent fields. In this paper, we focus on networks in which the underlying graph is a cycle graph. Based on a recent result on the maximum number of distinct frequency synchronization configurations in this context, we propose a constructive toric deformation homotopy method for locating all frequency synchronization configurations with complexity that is linear in this upper bound. Inspired by the polyhedral homotopy method for solving general polynomial systems and the more general framework of toric deformation in algebraic geometry, the proposed homotopy method deforms the set of synchronization configurations into a collection of toric varieties. Compared to existing homotopy methods for solving Kuramoto equations, the proposed method has the distinct advantages of avoiding the costly step of computing "mixed volume/cells" and using special starting systems that can be solved in linear time. We also explore the important consequences of this homotopy method in the context of directed acyclic decompositions of Kuramoto networks and tropical stable intersection points for Kuramoto equations.

**Keywords** Kuramoto model · Adjacency polytope · Polyhedral homotopy · Tropical geometry

#### 1 Introduction

A network of oscillators is a set of objects, varying between two states, that can influence one another. A network of N=n+1 oscillators can be modeled by a weighted graph G=(V,E,K) with the vertices  $V=\{0,\ldots,n\}$  representing the oscillators, the edges E representing the connections among the oscillators, and the weights  $K=\{k_{ij}\}$  representing the coupling strengths along the edges. Each oscillator i has a natural frequency  $c_i$ . In a network, however, oscillators influence one another and the dynamics can be described by the generalized Kuramoto model [29] given by the differential equations

$$\frac{d\theta_i}{dt} = c_i - \sum_{j \in \mathcal{N}_G(i)} k_{ij} \sin(\theta_i - \theta_j), \tag{1}$$

for i = 0, ..., n, where each  $\theta_i \in [0, 2\pi)$  is the phase angle that describes the state of the i-th oscillator, and  $\mathcal{N}_G(i)$  is the set of its neighbors. Here, we allow *non-uniform coupling strength*  $(k_{ij})$ 's may not be identical).

A fundamental mathematical problem in the study of the Kuramoto model as well as the behavior of

T. Chen

Department of Mathematics,

Auburn University Montgomery, Montgomery, AL, USA e-mail: ti@nranchen.org

R. Davis (⋈)

Department of Mathematics, Colgate University, Hamilton, NY, USA

e-mail: rdavis@colgate.edu

Published online: 04 June 2022



coupled oscillators is the occurrence of *synchronization*. Among many different notions of synchronization, this paper focuses only on *frequency synchronization*, which occurs when the competing forces of oscillators to stay with their natural frequency and the influence of their neighbors reach equilibrium for all oscillators, and they are all tuned to the same frequency. Then  $\frac{d\theta_i}{dt}=c$  for a common constant c for all i. They are precisely the solutions to the system of nonlinear equations

$$c_i - \sum_{j \in \mathcal{N}_G(i)} k_{ij} \sin(\theta_i - \theta_j) = c, \tag{2}$$

for i = 0, ..., n in the variables  $\theta_0, ..., \theta_n$ .

In this paper, we focus on the cases where the underlying graph is a cycle of N = n + 1 nodes so that the set E of edges of G consists of  $\{0, 1\}, \{1, 2\}, \ldots, \{n - 1, n\}, \{n, 0\}$ . This corresponds to a network of coupled oscillators in which each oscillator is influenced by exactly two adjacent oscillators. In [10], an upper bound on the total number of isolated solutions to the *synchronization equations* (2) is shown to be  $N\binom{N-1}{\lfloor (N-1)/2 \rfloor}$  using the theory of the birationally invariant intersection index. Indeed, this upper bound is generically sharp for a complexified version of (2). Recently, Lindberg, Zachariah, Boston, and Lesieutre [31] showed that this bound can also be attained by real solutions of (2).

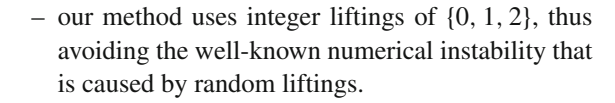
It is then natural to ask if there exists an algorithm that can locate all solutions of (2) with a complexity that is linear in this solution bound  $N\binom{N-1}{\lfloor (N-1)/2\rfloor}$ . This is the main topic that this paper addresses.

The primary contribution of this paper is the development of a homotopy method in the spirit of polyhedral homotopy (toric deformation) that will find *all* isolated solutions of (2). The total number of homotopy paths to be tracked with this method is exactly the solution bound

$$N\binom{N-1}{\lfloor (N-1)/2\rfloor},$$

where N = n + 1 is the number of oscillators in the cycle network. This method offers significant advantages over a direct application of polyhedral homotopy via the following features:

- our method avoids the costly step of computing mixed volumes or mixed cells;
- our method does not require solving binomial systems, and the starting systems can be solved in  $O(N^2)$  time in serial or O(N) time in parallel;



The secondary contribution is an explicit description of a regular unimodular triangulation of the adjacency polytope which significantly strengthens the previous volume and facet description results [10] and may shed new light on closely related constructions such as "symmetric edge polytopes" [16,22,24,39,40].

The tertiary contribution is our significant refinement for the directed acyclic decomposition scheme proposed in [7] for cycle graphs. This refined scheme is capable of reducing a network into simplest subnetworks known as primitive subnetworks for which frequency synchronization configurations can be computed both directly and efficiently. Finally, we provide an interpretation of our result in terms of tropical algebraic geometry as well as the equivalence of three rather different perspective to the Kuramoto equations.

The paper is organized as follows. In Sect. 2, we briefly review the Kuramoto model and the Kuramoto equations. Section 4 describes a complex algebraic formulation of the Kuramoto equations as a system of rational equations over the complex algebraic torus  $(\mathbb{C}^*)^n$ . Recent results on the generic root count of the algebraic Kuramoto equations, known as the adjacency polytope bound, is reviewed in Sect. 5. We strengthen this result by describing explicit formulas for a regular unimodular triangulation of the adjacency polytope in Sect. 6. The resulting algorithm is outlined in Sect. 7. Based on this triangulation, we develop our homotopy method in Sect. 8. In Sect. 9, we interpret our results in the broader context. An example is shown in Sect. 10, and the conclusion follows in Sect. 11. Software implementations are briefly described in "Code availability" section.

#### 2 Kuramoto equations and its variations

A simple mechanical analog of the coupled oscillator model (1) is a spring network, shown in Fig. 1, that consists of a set of weightless particles constrained to move on the unit circle without friction or collision [29]. The real numbers  $k_{ij} = k_{ji}$  characterizing the stiffness of the springs connecting particles i and j are known as *coupling strength*, and  $\frac{d\theta_i}{dt}$  represents the angular velocity of the i-th particle.



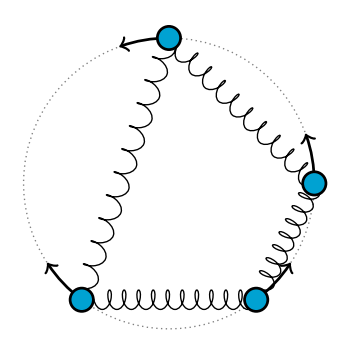


Fig. 1 A spring network

The class of special configurations in which the angular velocities of all particles can become perfectly aligned, that is, when  $\frac{d\theta_i}{dt} = c$  for  $i = 0, \ldots, n$  and a constant c, is known as the class of *frequency synchronization* configurations. By adopting a rotational frame of reference, we can always assume c = 0, i.e., frequency synchronization configurations are equivalent to equilibria of the ordinary differential equations (1). As a result of the symmetry assumption that  $k_{ij} = k_{ji}$ , the n+1 equilibrium equations must sum to zero. This allows the elimination of one of the equations, producing the system of n equations

$$c_i - \sum_{j \in \mathcal{N}_G(i)} k_{ij} \sin(\theta_i - \theta_j) = 0, \quad \text{for } i = 1, \dots, n$$

in the n unknowns  $\theta = (\theta_1, \dots, \theta_n)$ . The problem of finding some or all frequency synchronization configurations has been an active research topic in recent decades [5,14,15,21,26,33,35,38,43,44]. Traditionally, stable synchronization configurations or transition states (synchronization configurations with minimal unstable manifolds) are the main focus of studies. However, such configurations cannot be enumerated directly, and the most efficient and practical approach is still to find all synchronization configurations and selectively study a certain subset. Therefore, in this paper, we focus on the problem of finding all synchronization configurations.

Despite its mechanical origin, the above frequency synchronization system naturally appears in a long list of seemingly unrelated fields, including chemistry, electrical engineering, biology, and computer security. We refer to [17] for a detailed list. Here, we highlight two variations for which the method proposed in the present paper can be directly applied.

#### 2.1 Kuramoto model with phase shifts

In some applications, oscillators may be influenced by shifted phases of neighboring oscillators. Such phase shifts are characterized by symmetric parameters  $\{\delta_{ij}\}$ , and the generalized version of (3) is

$$c_i - \sum_{j \in \mathcal{N}_G(i)} k_{ij} \sin(\theta_i - \theta_j + \delta_{ij}) = 0, \tag{4}$$

for i = 1, ..., n. The presence of nonzero phase shift  $\{\delta_{ij}\}$  breaks the inherent symmetry of the model, yet the method developed here can directly handle such generalizations.

#### 2.2 Load-flow equations

With minor modifications, the system (2) can also be generalized to include a much broader family of models. Of particular interest in electric engineering are the load-flow equations. As a fundamental model in electric engineering, the load-flow equations describe the steady state of alternating current (AC) power networks.

The state of a power network consisting of nodes  $\{0,\ldots,n\}$  is defined by their complex voltages  $v_ie^{\mathbf{i}\theta_i}$  on the nodes  $i\in\{0,\ldots,n\}$ , where  $v_i\in\mathbb{R}^+$  represents the magnitude,  $\theta_i$  represents the phase, and  $\mathbf{i}$ , with  $\mathbf{i}^2=-1$ , is the imaginary unit. These voltages must satisfy balancing conditions derived from conservation laws. In particular, the real power balancing condition is given by the *load-flow* equations

$$P_{i} = \sum_{j} g_{ij} v_{i}^{2} - v_{i} v_{j} f_{ij} \sin(\theta_{i} - \theta_{j})$$
$$-g_{ij} \cos(\theta_{i} - \theta_{j})$$
 (5)

for each (non-slack) node i in the network, where  $g_{ij}$  is the conductance of the line connecting nodes i and j, while  $f_{ij}$  is its susceptance. With the assumptions that all nodes are modeled as generator nodes (PV buses), the  $v_i$  may be taken as constants, and the above equations are in the n unknowns  $\theta_1, \ldots, \theta_n$ .

This model differs from (6) in the presence of the cosine terms. As we shall demonstrate, the method developed here can be adapted to solve such generalizations. The algebraic formulation studied here is most directly related to the formulation used in [2]. An alternative method for analyzing load-flow equations derived from cycle networks was presented in [3].



#### 3 A toric deformation approach

In the rest of the paper, we will focus on the *Kuramoto equations* (2) with the understanding that all of the results can be directly applied to the generalizations described in Sects. 2.1 and 2.2. Our main goal is to develop a robust, efficient, and scalable method for solving these equations. In this section, we highlight the main idea behind the general approach that is the overarching framework of the present paper. The explanations here are provided to appeal to intuition, and the more rigorous formulation will be developed in Sect. 4.

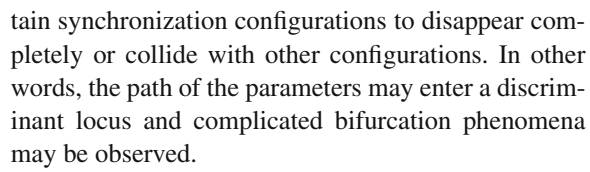
This approach starts with the viewpoint that the system (3) is actually a member of a family of similar systems parameterized by the coefficients  $k_{ij}$ , which is a viewpoint commonly adopted in the study of dynamical systems. Namely, we consider the family of systems of equations  $F(\theta_1, \ldots, \theta_n; t) = \mathbf{0}$ , given by

$$c_{i} - \sum_{j \in \mathcal{N}_{G}(i)} k_{ij}(t) \sin(\theta_{i} - \theta_{j}) = 0, \text{ for } i = 1, \dots, n,$$
(6)

parameterized by a real parameter t. Here, the functions  $k_{ij}(t)$  are defined so that  $\{k_{ij}(1)\}$  is the set of original coupling strengths. That is, the original equations (3) are the instance at t=1. The idea of introducing continuously varying parameters into a model is often used in studying the fundamental structure of solution sets, and it was proved to be a fruitful approach in the early study of the Kuramoto model. In the broader context of numerical computation, this idea is also the basis of a large class of numerical methods known as homotopy continuation methods.

The hope is that as t varies, the solutions  $(\theta_1, \ldots, \theta_n)$  to (6) also vary continuously in  $\mathbb{R}^n$ , forming continuous "solution paths" in  $\mathbb{R}^n \times \mathbb{R}$ . Under this assumption, we can move t to some value  $t_0$  at which the system (6) is particularly easy to solve. Once we find the solutions to  $F(\theta_1, \ldots, \theta_n; t_0) = \mathbf{0}$ , which are points on these solution paths, we can trace these paths and locate the solutions to the original system  $F(\theta_1, \ldots, \theta_n; 1) = \mathbf{0}$ .

This description is the naive view of a continuous deformation of the system (3). There are two obvious obstacles: first, there may be no choice of the parameter t at which the system  $F(\theta_1, \ldots, \theta_n; t) = \mathbf{0}$  is sufficiently easy to solve. Second, the solutions to  $F(\theta_1, \ldots, \theta_n; t) = \mathbf{0}$  may not move continuously as the parameter t varies, e.g., at certain choices of t, the resulting coupling strength  $\{k_{ij}(t)\}$  may cause cer-



Fortunately, both obstacles can be surmounted. The first requires introduction of additional structure, while second requires the extension of the complex state space and generic coefficients. In the following two subsections, we provide brief and informal explanations of these ideas. Finally, in Sect. 3.3, we consolidate these ideas into the formulation of a smooth deformation.

#### 3.1 Decoupling of bidirectional interaction terms

In the standard Kuramoto model, the interaction of two adjacent nodes i and j along the edge  $\{i, j\}$  is considered to be bidirectional and symmetric. We first generalize this view by decoupling this interaction into the two components along the directed edges (i, j) and (j, i), respectively. We define the *complex directed interaction function* along the directed edge (i, j) to be

$$z_{ij}(\boldsymbol{\theta}) = \frac{1}{2} [\sin(\theta_i - \theta_j) - \mathbf{i}\cos(\theta_i - \theta_j)]. \tag{7}$$

This function describes the interaction along the edge (i, j). On the other hand, the interaction along the opposite direction, i.e., the directed edge (j, i), is given by the function  $z_{ji}$ , as shown in Fig. 2 (see [7] for detail). The use of imaginary interaction terms is also the foundation of analytic Kuramoto models [36].

The imaginary part in  $z_{ij}$  is normally hidden in the sense that

$$z_{ij}(\boldsymbol{\theta}) - z_{ji}(\boldsymbol{\theta}) = \sin(\theta_i - \theta_j),$$

so that when both directed edges (i, j) and (j, i) are present, the combined effect reduces to the original

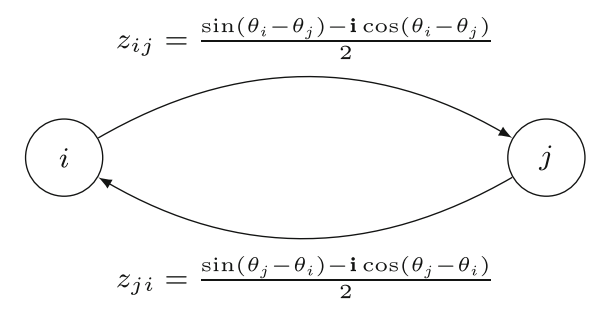


Fig. 2 Interactions along directed edges



interaction term in the standard Kuramoto model. Yet, the introduction of this hidden imaginary artifact provides additional structure through which much simpler systems can be produced via continuous deformation. In particular, with this notation, the original Kuramoto equation (2) can be written as

$$c_i - \sum_{j=0}^{n} (k_{ij} z_{ij} - k_{ji} z_{ji}) = 0$$
 for  $i = 1, ..., n$ ,

and the separation of the interaction term  $\sin(\theta_i - \theta_j)$  into two terms  $z_{ij}(\theta) - z_{ji}(\theta)$  allows the full decomposition of the equations [7]. The resulting system is sufficiently simple and can be solved directly.

#### 3.2 Allowing complex phase angles

The second ingredient needed to surmount our obstacles is the adoption of complex phase angles: instead of using only real phase angles  $\theta_i \in \mathbb{R}$ , we introduce imaginary parts  $\rho = (\rho_1, \ldots, \rho_n)$  as well as  $\rho_0 = 0$  and use  $\theta - \mathbf{i}\rho$  to represent the states of the oscillators. Of course, setting  $\rho = \mathbf{0}$  restores the original representations.

The extension to complex phase angles opens the door to leveraging complex analytical tools (e.g., the analytic Kuramoto model in [36]). In this paper, the use of complex phase angle is crucially important in ensuring that smooth deformation is possible. In Sect. 8, we will show, under a mild genericity assumption, that as the parameter t of (6) varies, the solutions  $\theta - i\rho$ , as complex phase angles, do indeed move continuously. This enables the fundamental idea of deformation.

# 3.3 Smooth deformation of models

Combining the ideas described in the subsections above, we can construct a family of generalized Kuramoto equations

$$c_i - \sum_{j \in \mathcal{N}_G(i)}^n [(k_{ij}t^{\omega_{ij}})z_{ij} - (k_{ji}t^{\omega_{ji}})z_{ji}] = 0$$
 (8)

for i = 1, ..., n, where the  $z_{ij}$  are complex valued functions of complex variables  $\theta - i\rho$ , and  $\{\omega_{ij}\}$  are positive constants to be carefully selected. When t = 1, the equation is identical to the original Kuramoto equation

(3). As *t* continuously varies from 1 toward 0, the coupling strengths are gradually decreased, and the generalized complex synchronization configurations also move continuously forming solution paths.

The constants  $\{\omega_{ij}\}$  are chosen carefully so that at the limit  $t \to 0$ , known as "toric infinity," the system breaks apart into particularly simple subsystems that can be solved directly, and their solutions provide us the starting points of the solution paths. From these starting points, we can employ robust numerical methods (known as path tracking algorithms) to track these paths and locate *all* synchronization configurations of the original model. Moreover, since each path produces at most one synchronization configuration, this idea also provides a practical way for counting the maximum number of synchronization configurations. We will review the root counting results in Sect. 5.

Identifying starting points of solution paths is the difficult part of this approach. Through the deep theory of toric algebraic geometry, this can be done through a special triangulation of a convex polytope, known as the adjacency polytope. Indeed, each cell in this triangulation produces a simple subsystem that (8) will be decomposed into at "toric infinity," which, in turn, produces a starting point of a solution path.

It is worth noting that not all deformation schemes are created equal. In previous work [7], the simple choice of a uniform constant  $\omega_{ij}$  leads to a coarse decomposition of the system "at toric infinity," which will require additional stages of further decomposition. One focus of this paper is a significant refinement of of this scheme through a special choice of the values of  $\{\omega_{ij}\}$ .

The next section sets up the rigorous algebraic formulation of the idea highlighted here.

#### 4 A complex algebraic formulation

To put the descriptions given in the previous section into a rigorous and algebraic form, we start with a complexification, which is crucial in applying the root counting results and homotopy continuation theory. Using the identity  $\sin(\theta_i - \theta_j) = \frac{1}{2i}(e^{i(\theta_i - \theta_j)} - e^{-i(\theta_i - \theta_j)})$ , the equations (3) can be transformed into

$$c_i - \sum_{j \in \mathcal{N}_G(i)} \frac{k_{ij}}{2\mathbf{i}} (e^{\mathbf{i}\theta_i} e^{-\mathbf{i}\theta_j} - e^{-\mathbf{i}\theta_i} e^{\mathbf{i}\theta_j}) = 0$$



for  $i=1,\ldots,n$ . We then extend the domain to the complex plane via  $\theta_i \mapsto \theta_i - \mathbf{i}\rho_i$  and introduce the change of variables  $x_i := e^{\mathbf{i}(\theta_i - \mathbf{i}\rho_i)} = e^{\rho_i + \mathbf{i}\theta_i}$  for  $i=1,\ldots,n$ . With these, the left-hand side of the above equation can be expressed as the Laurent polynomial

$$F_{G,i}(x_1,\ldots,x_n) = c_i - \sum_{j \in \mathcal{N}_G(i)} \left( a_{ij} \frac{x_i}{x_j} - b_{ij} \frac{x_j}{x_i} \right),$$
(9)

where  $a_{ij}$ ,  $b_{ij} = \frac{k_{ij}}{2\mathbf{i}}$ , and  $x_0 = 1$ .

Remark 1 If nonzero phase shift parameters  $\{\delta_{ij}\}$  (described in Sect. 2.1) are included, then  $a_{ij} = \frac{k_{ij}}{21}e^{\mathbf{i}\delta_{ij}}$  and  $b_{ij} = \frac{k_{ij}}{21}e^{-\mathbf{i}\delta_{ij}}$  will be different. Similarly, this formulation also includes the load-flow equations described in Sect. 2.2. In that case, we have  $a_{ij} = b_{ij} = \frac{f_{ij}}{2\mathbf{i}} + \frac{g_{ij}}{2}$ . Also note that the rational function  $\frac{x_i}{x_j}$  in the above equation corresponds to the complex interaction function  $z_{ij}(\theta)$  defined in (7).

A Laurent polynomial is simply a polynomial that may contain negative exponents of the variables, and we use the notation  $F_{G,i}$  to emphasize its dependence on the topology of the graph G. The system  $F_G$  =  $(F_{G,1},\ldots,F_{G,n})$  is thus a system of n Laurent polynomials in the *n* complex variables  $\mathbf{x} = (x_1, \dots, x_n)$ . In the following, it is referred to as the (algebraic) system of synchronization equations for a Kuramoto model, or simply a synchronization system. Since  $x_i$ 's appear in the denominators,  $F_G$  is only defined on the algebraic torus  $(\mathbb{C}^*)^n = (\mathbb{C} \setminus \{0\})^n$ . Each equivalence class of real solutions of (2), modulo translations by multiples of  $2\pi$ , corresponds to a single solution of (9) in  $(\mathbb{C}^*)^n$ . Conversely, only solutions  $(x_1, \ldots, x_n)$  with  $|x_i| = 1$ (i.e., on the unit circle of the complex plane) for each  $i = 1, \dots, n$  correspond to real solutions of the original synchronization equation (2). It is thus possible for this algebraic formulation to introduce extraneous solutions. However, as we shall summarize in Sect. 5, recent real root counting results shows that it is possible for *all* complex solutions of (9) to be real.

We now formulate the "unmixed" version of  $F_G$ , which will be the crucial construction that will allow us to introduce methods from convex geometry to this problem. If we consider  $F_G$  as a column vector, then for any nonsingular  $n \times n$  matrix R, the systems  $R \cdot F_G$  and  $F_G$  have the same zero set. Therefore, in the following,

it is sufficient to focus on the system

$$F_G^R = R \cdot F_G = \begin{bmatrix} r_{11} \cdots r_{1n} \\ \vdots & \ddots & \vdots \\ r_{n1} \cdots r_{nn} \end{bmatrix} \begin{bmatrix} F_{G,1} \\ \vdots \\ F_{G,n} \end{bmatrix}$$

It is easy to verify that for generic choices of the matrix R, there is no complete cancellation of the terms, and thus  $F_G^R$  is of the form

$$F_{G,k}^{R} = c_k^{R} - \sum_{\{i,j\} \in \mathcal{E}(G)} \left( a_{ijk}^{R} \frac{x_i}{x_j} + a_{jik}^{R} \frac{x_j}{x_i} \right) \tag{10}$$

for  $k = 1, \ldots, n$  where

$$c_k^R = r_{k1}c_1 + \dots + r_{kn}, c_n$$
$$a_{ijk}^R = r_{ki}a_{ij} - r_{kj}b_{ji}$$

are the resulting nonzero coefficients after collection of similar terms. Every equation in this system has the same set of monomials, and such systems are known as *unmixed* systems. Thus, the system (10) will be referred to as the *unmixed form* of the synchronization equations, and it will be the main focus of the rest of this paper.

#### 5 Maximum and generic root count

In this section, we briefly review the existing results on the root counts of (2), (9), and (10).

In [2], an upper bound on the number of equilibria of the Kuramoto model (solutions to (2)) induced by a graph of N vertices with any coupling strengths is shown to be  $\binom{2N-2}{N-1}$ . This bound can be understood as a bi-homogeneous Bézout number on the algebraic version (9) or (10): via the map  $y_i = x_i^{-1}$ , the two systems can be translated into equivalent systems that have a bi-degree of (1, 1) with respect to the partition and are defined in  $((x_1, \ldots, x_n), (y_1, \ldots, y_n))$  with the additional conditions that  $x_i y_i = 1$  for  $i = 1, \ldots, n$ . It is easy to verify that the bi-homogeneous Bézout number will be  $\binom{2n}{n} = \binom{2(N-1)}{N-1}$ .

Recent studies [12] suggest tighter bounds on the number of isolated complex solutions may exist when the network is sparsely connected. When the underlying graph is a cycle, a sharp bound is established in [10] using the theory of the birationally invariant intersection index as well as a construction known as the adjacency polytope which we shall review briefly here.



Recall that a polytope is a bounded intersection of finitely many closed half-spaces. For any polytope, there is a finite set *S* for which the polytope is the *convex hull* of *S*, that is, the smallest convex set containing *S*; we use the notation conv *S* to denote the convex hull of *S*.

The adjacency polytope in particular is a polytope that encodes the topological information of the Kuramoto network. Given an undirected graph G with edge set  $\mathcal{E}(G)$ , its *adjacency polytope* is defined to be

$$P_G = \operatorname{conv}\left\{\mathbf{e}_i - \mathbf{e}_j \mid \{i, j\} \in \mathcal{E}(G)\right\}$$
 (11)

where we adopt the convention that  $\mathbf{e}_0 = \mathbf{e}_{n+1} = \mathbf{0}$ . That is, the adjacency polytope of G is the convex hull of a set of line segments, each corresponding to an edge in G. Note  $P_G$  is a *lattice polytope* in the sense that all of its vertices have integer coordinates. Similar constructions have also appeared in other contexts (e.g., [16,23,34]).

The adjacency polytope bound [8] of a Kuramoto system (2) on the graph G is defined to be the normalized volume of  $P_G$ , which is  $n! \operatorname{vol}(P_G)$ . This bound is an upper bound for the number of isolated complex solutions for the systems (9) and (10). Consequently, it is also an upper bound for the number of real solutions that the original synchronization system (2) has.

In the case of a cycle graph of N nodes, i.e., the graph  $G = C_N$  with edge set  $\{\{0, 1\}, \dots, \{N-2, N-1\}, \{N-1, 0\}\}$ , the recent paper [10] establishes the explicit formula  $N\binom{N-1}{\lfloor (N-1)/2\rfloor}$  for the adjacency polytope bound. Furthermore it is shown that this bound coincides with the birationally invariant intersection index in  $(\mathbb{C}^*)^n$  of the Kuramoto system (9) as a member of a family of rational functions. This result is strengthened significantly by Lindberg, Zachariah, Boston, and Lesieutre [31], who showed that this bound can also be attained by real solutions of (2).

In this paper, we further extend this theoretical framework by producing an explicit construction of a unimodular triangulation of the adjacency polytope for cycle graphs and define a homotopy method based on this triangulation.

Before continuing, two remarks are in order.

Remark 2 The theory of the birationally invariant intersection index [27,28] (as well as the general intersection theory [18] and homotopy continuation theory [30,42]) shows that the adjacency polytope bound is "generically exact" in the sense that if one chooses the

coefficients of the algebraic Kuramoto equations (9) randomly then, with probably one, the total number of isolated complex solutions that system has is exactly the adjacency polytope bound  $N\binom{N-1}{\lfloor (N-1)/2 \rfloor}$ . Stated more precisely, there exists a nonzero polynomial D whose variables are the coefficients  $\{c_i\}$  and  $\{a_{ij}\}\$  of (10) such that for all choices of  $\{c_i\}$  and  $\{a_{ij}\}$  where  $D \neq 0$ , the total number of isolated complex roots of (9) reaches the adjacency polytope bound. What is particularly remarkable is that the adjacency polytope bound (the generic root count of (10)), the Bernstein-Kushnirenko-Khovanskii bound (the generic root count of (9)), the most refined birationally invariant intersection index, and even the maximum real root count of (2) are all identical. This shows that the sequence of relaxations (from the original real transcendental equations (3) to the algebraic formulation (9) and then to its unmixed version (10)) does not necessarily introduce extraneous solutions.

Remark 3 In specific cases, the adjacency polytope of a graph on  $\{0, \ldots, N-1\}$  coincides with the type  $A_{N-1}$  root polytope as defined in [1]. This polytope is defined as the convex hull of the generators in  $\mathbb{Z}^N$  of the root lattice, generated as a monoid, of the Coxeter group of type  $A_{N-1}$ . Indeed, this is exactly the adjacency polytope  $P_G$  where G is the graph for which 0 is an isolated vertex and the induced subgraph on  $\{1, \ldots, N-1\}$  is  $K_{N-1}$ . However, in the type  $C_{N-1}$  and type  $D_{N-1}$  cases, the constructions of the root polytopes do not coincide with any adjacency polytopes.

One should take care when researching root polytopes in the literature, as there are competing notions of root polytopes for root lattices of type  $A_{N-1}$ . One is as we have mentioned, while another considers only *positive* roots of the root lattice (and the origin). This root polytope was introduced and studied in [41, Section 12], with an emphasis on connections to the broad class of polytopes called *generalized permutohedra*.

# 6 A regular, unimodular triangulation of the adjacency polytope

From the informal idea of deformation discussed in Sect. 3.3, we will formulate a concrete numerical homotopy method for solving the synchronization equations. One important ingredient in this construction is a "regular and unimodular triangulation" of the



adjacency polytope (defined in (11)). Indeed, each cell in this triangulation gives rise to a solution path that will reach one complex solution to (9). In this section, we describe this triangulation in detail.

A *subdivision* of an *n*-dimensional polytope P is a collection of polytopes  $P_1, \ldots, P_k \subseteq P$  such that

- 1. dim  $P_i = n$  for all i,
- 2.  $P_i \cap P_j$  is either empty or a face common to both  $P_i$  and  $P_j$ , and
- 3.  $P = \bigcup_i P_i$ .

A *triangulation*, a.k.a. *simplicial subdivision*, of a polytope is a subdivision consisting entirely of simplices. Furthermore, a triangulation is said to be *unimodular* if all of the member simplices are lattice simplices of normalized volume 1.

In order to be used in our homotopy construction, the "regularity" property of the triangulation is also required. Recall that a *facet* of a polytope is a face of codimension 1. A triangulation of a polytope is said to be *regular* if it is the projection of the lower facets of a lifting of the polytope into one-higher dimension. More precisely, given a polytope  $P = \text{conv}\{\mathbf{v}_1, \dots, \mathbf{v}_m\}$  in  $\mathbb{R}^n$  and weights  $\omega_1, \dots, \omega_m \in \mathbb{R}$ , the new polytope

$$P' = \operatorname{conv}\{(\mathbf{v}_i, \omega_i) \in \mathbb{R}^{n+1} \mid i = 1, \dots, m\}$$

is a lifting of P into one-higher dimension. The projections of *lower facets*, that is, the facets whose inner normal vectors have positive last entry, to the first n coordinates is called a *regular subdivision*, or a *regular triangulation* if all facets are simplices.

Remark 4 We note that the lifting into one-higher dimension corresponds to the introduction of the additional parameter t in (6).

For the rest of this paper, we shall fix the graph to be  $G = C_N$ , the cycle graph  $C_N$  on N = n + 1 nodes. We will construct a unimodular triangulation for the adjacency polytope  $P_{C_N}$  by finding and triangulating all of its facets. Using the set of facets  $\mathcal{F}(P_{C_N})$ , a well-known subdivision of  $P_{C_N}$  can be constructed as the set of pyramids formed by the facets and a fixed interior point as the common apex. That is, fixing any interior point  $\mathbf{p} \in P_{C_N}$ , the set

$$\{\operatorname{conv} F \cup \{\mathbf{p}\} \mid F \in \mathcal{F}(P_{C_N})\}$$

forms a subdivision of  $P_{C_N}$ . By further triangulating each facet, the above subdivision can be refined into a

triangulation of  $P_{C_N}$ . That is, if T(F) is a triangulation of the facet  $F \in \mathcal{F}(P_{C_N})$  then the set

$$\{\operatorname{conv} C \cup \{\mathbf{p}\} \mid C \in T(F), F \in \mathcal{F}(P_{C_N})\}$$

for a fixed interior point **p** form a triangulation of  $P_{C_N}$ . This is the strategy that we will follow in this section. The choice of the interior point **p** will be the origin **0** which is an interior point of  $P_{C_N}$  since it is the average of  $\mathbf{e}_i - \mathbf{e}_j$  and  $\mathbf{e}_j - \mathbf{e}_i$  for all edges  $\{i, j\}$ .

It was shown in [10] that  $P_{C_N}$  is unimodularly equivalent to the polytope

$$Q_N = \operatorname{conv}\{\pm \mathbf{e}_1, \dots, \pm \mathbf{e}_n, \pm (\mathbf{e}_1 + \dots + \mathbf{e}_n)\}\$$

via the map  $x \mapsto Ax$ , where A is the  $n \times n$  matrix with 1 on and below the diagonal and 0 everywhere else. Then, [10, Proposition 12] and [37, Remark 4.3] identify the facets of  $Q_N$ . The geometric structure of this polytope depends on the parity of N. When N is even, the facets can be indexed by the set

$$\Lambda_N = \left\{ (\lambda_1, \dots, \lambda_N) \in \{-1, 1\}^N \mid \sum_{i=1}^N \lambda_i = 0 \right\},\,$$

and for each  $\lambda = (\lambda_1, \dots, \lambda_N) \in \Lambda_N$ , the corresponding facet is of the form

$$F_{\lambda} = \text{conv}\{\lambda_1(-\mathbf{e}_1 - \mathbf{e}_2 - \dots - \mathbf{e}_n), \lambda_2\mathbf{e}_1, \dots, \lambda_N\mathbf{e}_n, \}.$$

When *N* is odd, we define  $\Lambda_N$  differently: in this case, the facets can be indexed by  $\Lambda_N := \bigcup_{i=1}^N \Lambda_{j,N}$  where

$$\Lambda_{j,N} = \left\{ (\lambda_1, \dots, \lambda_N) \middle| \begin{array}{l} \lambda_i \in \{-1, 1\} \text{ for all } i \neq j, \\ \lambda_j = 0, \lambda_1 + \dots + \lambda_N = 0 \end{array} \right\},$$

and the facet corresponding to  $\lambda = (\lambda_1, ..., \lambda_N) \in \Lambda_{j,N}$  is given by

$$F_{\lambda} = \operatorname{conv} \left\{ \begin{array}{l} \lambda_1(-\mathbf{e}_1 - \mathbf{e}_2 - \dots - \mathbf{e}_n), \\ \lambda_2 \mathbf{e}_1, \dots, \widehat{\lambda_j \mathbf{e}_{j-1}}, \dots, \lambda_N \mathbf{e}_n \end{array} \right\}.$$

Here, the notation  $\lambda_j \mathbf{e}_{j-1}$  indicates that element is excluded from the list.

From the above constructions, we can see that  $Q_N$  is *simplicial*, i.e., all the facets are simplices, when N is odd, but is not simplicial when N is even. Via the unimodular equivalence between  $Q_N$  and  $P_{C_N}$  we have same characterization of the facets of  $P_{C_N}$ . As a result of this dichotomy, the constructions of the triangulations in the even and odd N cases require very different procedures.

Remark 5 (Unimodular equivalence of facets) Another important property worth noting is that the facets of



 $Q_N$  are all unimodularly equivalent to each other. To see this suppose  $F_{\lambda}$ ,  $F_{\lambda'}$  are facets of  $Q_N$ . Then  $F_{\lambda'}=f(F_{\lambda})$  where  $f(x)=B_{\lambda,\lambda'}x$  and  $B_{\lambda,\lambda'}$  is the  $n\times n$  matrix constructed as follows: first let  $\ell=\lambda_1\lambda_1'$ . For  $1\leq i\leq n$ , note that there is a unique j such that  $\lambda_{i+1}$  is the  $j^{th}$  instance of -1 or the  $j^{th}$  instance of 1 in  $(\lambda_2,\ldots,\lambda_N)$ . Let  $\ell\lambda_{k+1}'$  be the  $j^{th}$  instance of  $\ell\lambda_{i+1}$  in  $(\ell\lambda_2',\ldots,\ell\lambda_N')$ . Set row  $\ell$  of  $\ell$  of  $\ell$  in  $\ell$  in

Consider, for example, the case with N=3 and the choices of  $\lambda=(1,-1,-1,1)$  and  $\lambda'=(-1,1,-1,1)$ . In this case,  $\ell=\lambda_1\lambda_1'=-1$ . Note that  $\lambda_2$  is the first instance of -1 in  $(\lambda_2,\lambda_3,\lambda_4)$ . Now,  $-\lambda_2'$  is the first occurrence of  $-\lambda_2$  in  $(-\lambda_2',-\lambda_3',-\lambda_4')$ . So, the first row of  $B_{\lambda,\lambda'}$  is  $-\mathbf{e}_1$ . Next,  $\lambda_3$  is the second occurrence of -1 in  $(\lambda_2,\lambda_3,\lambda_4)$ , and  $-\lambda_4'$  is the second occurrence of -1 in  $(-\lambda_2',-\lambda_3',-\lambda_4')$ , so the second row of  $B_{\lambda,\lambda'}$  is  $-\mathbf{e}_3$ . Since  $\lambda_3$  is the first occurrence of 1 in  $(\lambda_2,\lambda_3,\lambda_4)$ , and  $-\lambda_3'$  is the first occurrence of 1 in  $(-\lambda_2',-\lambda_3',-\lambda_4')$ , we have that the third row of  $B_{\lambda,\lambda'}$  is  $-\mathbf{e}_2$ :

$$B_{\lambda,\lambda'} = \begin{bmatrix} -1 & 0 & 0 \\ 0 & 0 & -1 \\ 0 & -1 & 0 \end{bmatrix}.$$

Remark 6 (Point configuration) In order to be used in a homotopy construction, a stronger triangulation is needed. Define the point set

$$S_{C_N} = \{\mathbf{0}\} \cup \{\mathbf{e}_i - \mathbf{e}_j \mid \{i, j\} \in \mathcal{E}(C_N)\}$$

This set is known as the *support* of the unmixed system (10) as it collects the exponents (as points) of all of the terms appearing in that system. It is easy to see that  $P_{C_N} = \text{conv } S_{C_N}$  since  $\mathbf{0}$  is an interior point of  $P_{C_N}$  (as  $\mathbf{0} = \frac{1}{2}(\mathbf{e}_i - \mathbf{e}_j) + \frac{1}{2}(\mathbf{e}_j - \mathbf{e}_i)$ ). In our constructions, we will require all simplices in a triangulation to have vertices within the set  $S_{C_N}$ . This is known as a triangulation of a *point configuration*.

In the rest of this section, we describe the construction of regular unimodular triangulation of  $P_{C_N}$  in the cases with even and odd N, respectively.

#### 6.1 Even N

For the entirety of this subsection, we assume that N is even. From the preceding discussion, we know that all

of the facets of  $P_{C_N}$  are unimodularly equivalent due to transitivity of equivalence relations. In particular, all facets of  $P_{C_N}$  are unimodularly equivalent to

$$\operatorname{conv}\left\{ \begin{aligned} & e_0 - e_1, e_1 - e_2, \dots, e_{\lfloor \frac{n}{2} \rfloor} - e_{\lfloor \frac{n}{2} \rfloor + 1}, \\ & - (e_{\lfloor \frac{n}{2} \rfloor + 1} - e_{\lfloor \frac{n}{2} \rfloor + 2}), \dots, - (e_{n-1} - e_n), - e_n \end{aligned} \right\}$$

Let  $G_{\lambda}$  denote the facet of  $P_{C_N}$  obtained by applying  $A^{-1}$  to all points in  $F_{\lambda}$ . It will be important to keep in mind that  $\pm A^{-1}(\mathbf{e}_1 + \cdots + \mathbf{e}_n) = \pm \mathbf{e}_1$ . We can then produce a subdivision of  $P_{C_N}$  by setting

$$G_{\lambda}^{0} = \operatorname{conv}\{0, G_{\lambda}\}.$$

and ranging overall  $\lambda \in \Lambda_N$ .

To aid us in what follows, we establish the following lemma. Recall that in  $\mathbb{R}^n$ , we use the convention  $\mathbf{e}_0 = \mathbf{e}_{n+1} = \mathbf{0}$ .

**Lemma 7** Let  $V_N = \{\mathbf{v}_0, \dots, \mathbf{v}_N\}$  denote the vertices of  $G_1^0$  such that

$$\mathbf{v}_i = \begin{cases} \mathbf{0} & \text{if } i = 0, \\ \lambda_i(\mathbf{e}_{i-1} - \mathbf{e}_i) & \text{if } 1 \le i \le N, \end{cases}$$

If N is even, then each  $G_{\lambda}^{0}$  has exactly two triangulations:

$$\Delta_{+}(G_{\lambda}^{0}) = \{\operatorname{conv}\{V_{N} \setminus \{\mathbf{v}_{i}\}\} \mid \lambda_{i} = \lambda_{1}\}\$$

and

$$\Delta_{-}(G_{\lambda}^{0}) = \{\operatorname{conv}\{V_{N} \setminus \{\mathbf{v}_{i}\}\} \mid \lambda_{i} = -\lambda_{1}\}.$$

Moreover, both of these triangulations are regular.

**Proof** Let N=2k. Note that for each  $\lambda \in \Lambda_N$ , dim  $G_{\lambda}^{0}=n$  and  $G_{\lambda}^{0}$  has n+2 vertices. Thus, there is a unique (up to simultaneous scaling of the coefficients) affine dependence of the form

$$\sum_{i=0}^{N} c_i \mathbf{v}_i = \mathbf{0}$$

satisfying  $\sum c_j = 0$  with  $c_0, \ldots, c_{n+1} \in \mathbb{R}$ . Without loss of generality, we may choose  $c_0 = 0$  and  $c_i = \lambda_i k/N$  for i > 0.

The desired conclusions for the lemma then follow from [13, Lemma 2.4.2]. Specifically,

$$\Delta_{+}(G_{1}^{0}) = \{\operatorname{conv}\{V \setminus \{\mathbf{v}_{i}\}\} \mid \lambda_{i} = \lambda_{1}\}$$

is the triangulation of  $G_{\lambda}^{0}$  corresponding to the height vector  $(\omega_0, \ldots, \omega_N)$  where

$$\omega_i = \begin{cases} 0 & \text{if } c_i \le 0, \\ 1 & \text{if } c_i > 0 \end{cases}$$



and

$$\Delta_{-}(G_{\lambda}^{0}) = \{\operatorname{conv}\{V \setminus \{\mathbf{v}_{i}\}\} \mid \lambda_{i} = -\lambda_{1}\}$$

is the triangulation corresponding to the heights

$$\omega_i = \begin{cases} 0 & \text{if } c_i \ge 0, \\ 1 & \text{if } c_i < 0. \end{cases}$$

We will be concerned with the particular lifting function  $\omega: S_{C_N} \to \mathbb{Z}$  given by

$$\omega(\mathbf{a}) = \begin{cases} 0 & \text{if } \mathbf{a} = \mathbf{0} \\ 2 & \text{if } \mathbf{a} = \pm \mathbf{e}_1 \\ 1 & \text{otherwise} \end{cases}$$

as this will induce the desired regular, unimodular triangulation  $\Delta_N$  of  $P_{C_N}$ . To help us with notation, we will define

$$\Omega_{\omega}(P) = \operatorname{conv}\{\omega(v) \mid v \in P \cap S_{C_N}\}\$$

for any polytope P whose vertices are a subset of  $S_{C_N}$ . If X is a collection of polytopes whose vertices are subsets of  $S_{C_N}$ , then we let  $\Omega_{\omega}(X) = \{\Omega_{\omega}(P) \mid P \in X\}$ .

First, we will identify the normal vectors of simplices in  $\Omega_{\omega}(\Delta_{+}(G_{\lambda}^{\mathbf{0}}))$ . Recall that a vector is *upward-pointing* if its final coordinate is positive.

**Lemma 8** Let N be even. If  $\lambda \in \Lambda_N$  and  $\lambda_1 = 1$ , then the upward-pointing inner normal vectors for all simplices in  $\Omega_{\omega}(\Delta_{+}(G^{\mathbf{0}}_{\lambda}))$  are  $x_{\lambda} = (x_1, \dots, x_{n+1})$  where

$$x_i = \begin{cases} \sum_{j=1}^{i} \lambda_j & \text{if } 1 \le i < n+1, \\ 1 & \text{if } i = n+1 \end{cases}$$

as well as

$$y_{\lambda,j} = x + \sum_{k=1}^{j-1} \mathbf{e}_k$$

for each j > 1 such that  $\lambda_j = 1$ . If  $\lambda_1 = -1$ , then the upward-pointing inner normal vectors are  $x_{\lambda} = \sigma(x_{-\lambda})$ ,  $y_{\lambda,j} = \sigma(y_{-\lambda,j})$  where  $\lambda_j > 0$  and where  $\sigma$  is the map that negates the first n coordinates.

*Proof* First observe that by construction, each vector under consideration is upward-pointing. Next, let  $\lambda_1 = 1$ . It is then straightforward to verify that

$$\langle \mathbf{x}, \lambda_i (\mathbf{e}_{i-1} - \mathbf{e}_i) + \mathbf{e}_{n+1} \rangle = -\lambda_i^2 + 1 = 0$$



for all  $1 < j \le n+1$ . Following this same process, one may verify that the hyperplane for which  $y_{\lambda,j}$  is normal contains all vertices of  $G_{\lambda}^{0}$  except  $\lambda_{j}(\mathbf{e}_{j-1} - \mathbf{e}_{j})$ .

Finally, notice that if  $\lambda' = -\lambda$ , then  $-T \in \Delta_+(G_{\lambda'}^0)$  for each cell  $T \in \Delta_+(G_{\lambda}^0)$ . It directly follows that  $\sigma(x_{\lambda})$  and  $\sigma(y_{\lambda,j})$  are the upward-pointing inner normal vectors of the simplices in  $\Delta_+(G_{\lambda}^0)$  for all  $\lambda$  satisfying  $\lambda_1 = -1$ .

**Theorem 9** Let N be even. The lifting function  $\omega$ :  $S_G \to \mathbb{Z}$  given by

$$\omega(\mathbf{a}) = \begin{cases} 0 & \text{if } \mathbf{a} = \mathbf{0}, \\ 2 & \text{if } \mathbf{a} = \pm e_1, \\ 1 & \text{otherwise} \end{cases}$$
 (12)

induces a regular unimodular triangulation  $\Delta_N$  of the point configuration  $S_{C_N}$ . Specifically,

$$\Delta_N = \bigcup_{\lambda \in \Lambda_N} \Delta_+(G_\lambda^0) \tag{13}$$

*Proof* Let  $\Delta_N$  denote the regular subdivision of  $P_{C_N}$  induced by  $\omega$ . For  $\lambda \in \Lambda_N$ , consider the vectors  $x_\lambda$ ,  $y_{\lambda,j}$ ,  $\sigma(x_\lambda)$ ,  $\sigma(y_{\lambda,j})$ , as defined in Lemma 8. First, we focus on  $x_\lambda$ . We have already seen that each vertex of  $G_\lambda^0$  except for  $-\lambda_1 e_1$  lies on the hyperplane with normal vector x. In fact, it is straightforward to check that

$$\langle x, -\lambda_i(\mathbf{e}_{i-1} - \mathbf{e}_i) + \mathbf{e}_{n+1} \rangle = \lambda_i^2 + 1 > 0$$

for all  $1 < j \le n + 1$ , and that

$$\langle x, \pm \mathbf{e}_1 + 2\mathbf{e}_{n+1} \rangle = \pm 1 + 2 > 0,$$

so x defines a facet of  $\Omega_{\omega}(P_{C_N})$ .

Following this same process, one may verify that  $y_{\lambda,j}$  defines a facet containing all vertices of  $G_{\lambda}^{0}$  except  $\lambda_{j}(\mathbf{e}_{j-1}-\mathbf{e}_{j})$ . By an argument that is symmetric in the first n coordinates,  $\sigma(x_{\lambda})$  and  $\sigma(y_{\lambda,j})$  also define facets of  $\Omega_{\omega}(P_{C_{N}})$ .

Ranging overall  $\lambda \in \Lambda_N$ , we have identified a collection of simplices C that are lower facets of  $\Omega_{\omega}(P_{C_N})$ . Projecting each C back down to  $\mathbb{R}^n$ , we get

$$\bigcup_{\lambda \in \Lambda_N} \Delta_+(G_\lambda^{\mathbf{0}}) \subseteq \Delta_N. \tag{14}$$

In fact, this set covers  $P_{C_N}$  completely: let  $a \in P_{C_N}$ . Then for some nonzero  $c \in \mathbb{R}$ , ca is on the boundary of  $P_{C_N}$ . Thus,  $ca \in G_{\lambda}$  for some  $\lambda \in \Lambda_N$ , and  $a \in G_{\lambda}^{\mathbf{0}}$ . Therefore,  $a \in C$  for some cell  $C \in \Delta_+(G_{\lambda}^{\mathbf{0}})$ .

Together, this shows that  $\Delta_N$  is a triangulation of  $P_{C_N}$ , and is the regular triangulation induced by  $\omega$ . To

see that this triangulation is unimodular, recall that all simplices in  $\Delta_N$  are unimodularly equivalent to the simplex whose nonzero vertices are

$$\mathbf{e}_0 - \mathbf{e}_1, \mathbf{e}_1 - \mathbf{e}_2, \dots, \mathbf{e}_{\lfloor \frac{n}{2} \rfloor} - \mathbf{e}_{\lfloor \frac{n}{2} \rfloor + 1}, \\ -(\mathbf{e}_{\lfloor \frac{n}{3} \rfloor + 1} - \mathbf{e}_{\lfloor \frac{n}{3} \rfloor + 2}), \dots, -(\mathbf{e}_{n-1} - \mathbf{e}_n), -\mathbf{e}_n.$$

Placing these vertices as the columns of a matrix, in this order, results in a lower-triangular matrix with determinant  $\pm 1$ . Thus, the corresponding simplex, and therefore all simplices in  $\Delta_N$ , are unimodular. This completes the proof.

Remark 10 The directed acyclic decomposition scheme developed in [7] is equivalent to the process of computing a regular subdivision of the adjacency polytope induced by certain 0/1 weights. It is shown that for certain graphs, this process will produce regular unimodular triangulations, which is desired due to their connection to primitive decomposition of a Kuramoto network. Here, however, we can see this is not possible in general. In particular, with the aid of Macaulay2 [20] to test all  $2^9 = 512$  possible 0/1 weight orders for  $P_{C_4}$ , we verified that only 4 choices of weights produce a triangulation of the polytope, and of these, none are unimodular. So, in the sense of bounding, the heights of the lattice points of  $\omega(P_{C_N})$  for all even N, using only nonnegative integer heights, to produce a regular unimodular triangulation, the  $\omega$  given in this subsection is best possible.

#### 6.2 Odd N

For the entirety of this subsection, we assume that N is odd. Recall that in this case, the facets of  $Q_N$  consist of all sets of the form

$$F_{j,\lambda} = \operatorname{conv} \left\{ \begin{array}{l} \lambda_1(-\mathbf{e}_1 - \mathbf{e}_2 - \dots - \mathbf{e}_n), \\ \widehat{\lambda_2} \mathbf{e}_1, \dots, \widehat{\lambda_j} \mathbf{e}_{j+1}, \dots, \lambda_N \mathbf{e}_n \end{array} \right\}$$

Tracing this back to  $P_{C_N}$ , we find that its facets are of the form

$$G_{\lambda} = \operatorname{conv} \left\{ \begin{array}{c} \lambda_{1}(\mathbf{e}_{0} - \mathbf{e}_{1}), \lambda_{2}(\mathbf{e}_{1} - \mathbf{e}_{2}), \dots, \\ \lambda_{j}(\widehat{\mathbf{e}_{j-1}} - \mathbf{e}_{j}), \dots, \lambda_{N}(\mathbf{e}_{n} - \mathbf{e}_{N}) \end{array} \right\}$$

for  $\lambda \in \Lambda_{j,N}$ . Set

$$G_{\lambda}^{\mathbf{0}} = \operatorname{conv}\{\lambda_i(\mathbf{e}_i - \mathbf{e}_{i+1}) \mid (\lambda_1, \dots, \lambda_N) \in \Lambda_{j,N}\},\$$

and let

$$\Delta_N = \{ G_\lambda^0 \mid \lambda \in \Lambda_N \}. \tag{15}$$

By construction, since each  $G_{\lambda}$  is a simplex,  $\Delta_N$  is a triangulation of  $P_{C_N}$ . It is straightforward to check that the matrix whose columns are the nonzero vertices of  $G_{\lambda}^{0}$  has determinant  $\pm 1$  for each  $\lambda \in \Lambda_N$ , so  $\Delta_N$  is a unimodular triangulation.

Let  $\omega: S_{C_N} \to \mathbb{Z}$  be the height function given by

$$\omega(\mathbf{a}) = \begin{cases} 0 & \text{if } \mathbf{a} = \mathbf{0} \\ 1 & \text{otherwise.} \end{cases}$$
 (16)

It is clear from this choice that the lower facets of the lifted polytope  $\Omega_{\omega}(P_{C_N})$  are of the form

$$\operatorname{conv}\{\mathbf{0}, G_{\lambda} \times \{1\}\},\$$

so their projections back onto  $\mathbb{R}^n$  are exactly the simplices  $G^0_{\lambda}$  for all  $\lambda \in \Lambda_N$ . With this work, we have shown the following.

**Proposition 11** The set  $\Delta_N$  is a regular, unimodular triangulation of  $P_{C_N}$ , and is induced by the lifting function  $\omega$  in (16).

We can, in fact, be more specific when identifying the lower facets of  $\Omega_{\omega}(P_{C_N})$ .

**Corollary 12** The upward-pointing inner normal vectors for  $\Omega_{\omega}(G_{\lambda}^{\mathbf{0}})$  are  $x = (x_1, \dots, x_N)$  where

$$x_k = \begin{cases} \sum_{i=1}^k \lambda_i & \text{if } i < N, \\ 1 & \text{if } i = N \end{cases}$$

for all  $\lambda \in \Lambda_N$ .

Proof Let  $\Omega_{\omega}(G_{\lambda}^{0})$  be a lower facet of  $\Omega_{\omega}(P_{C_{N}})$  for some  $\lambda \in \Lambda_{j,N}$ , and select a nonzero vertex **v** of the facet. Since this vertex is nonzero, we know **v** is of the form  $\mathbf{v} = \lambda_{r+1}(\mathbf{e}_{r} - \mathbf{e}_{r+1} + \mathbf{e}_{N})$  for some  $r \neq j$ . Then,

$$\langle \mathbf{x}, \mathbf{v} \rangle = \lambda_{r+1} \left( \sum_{i=1}^r \lambda_i - \sum_{l=1}^{r+1} \lambda_l \right) + 1 = -\lambda_{r+1}^2 + 1 = 0.$$

Thus, **x** is normal to  $\Omega_{\omega}(G_{\lambda}^{\mathbf{0}})$ .

## 7 Cell enumeration algorithm

In this section, we briefly summarize the algorithm for constructing a regular unimodular triangulation for the adjacency polytope  $P_{C_N}$  as proposed above. Here, we shall focus only on the enumeration of all the upward pointing inner normal vectors of the lifted polytope  $\Omega(P_{C_N})$  of the point configuration  $S_{C_N}$ , since these



are directly used in the homotopy construction to be described in Sect. 8. Moreover, these objects directly correspond to tropical stable intersections as we shall discuss in detail in Sect. 9.2. Once a normal vector  $\mathbf{v}$  is obtained, the vertices of the corresponding cell can be found easily by computing the minimizing set of the linear functional  $\langle \cdot , \mathbf{v} \rangle$ .

The algorithm EnumerateNormals(N) for enumerating inner normal vectors is listed in Algorithm 1. It takes the argument N, which is the number of nodes in the cycle graph, and produces the upward-pointing inner normal vectors of the lower facets of  $\Omega(P_{C_N})$  which are in one-to-one correspondence with the simplices in the regular unimodular triangulation  $\Delta_N$ .

**Algorithm 1** EnumerateNormals(*N*): Enumeration of upward pointing inner normals

```
Input: N \in \mathbb{Z}^+, N > 2.
Output: Set C of all upward pointing inner normals.
   C \leftarrow \emptyset
   for all (\lambda_1, \ldots, \lambda_n) \in \Lambda_N do
       for k = 1, ..., n do
x_k \leftarrow \sum_{i=1}^k \lambda_i
       end for
       x_N \leftarrow 1
       \mathbf{x} \leftarrow [x_1, \dots, x_N]
       C \leftarrow C \cup \{\mathbf{x}\}\
       if N is even and N > 2 then
           for j = 1, ..., n do
              if \lambda_i = 1 then
                  \mathbf{y} \leftarrow \mathbf{x} + \sum_{k=1}^{j-1} \mathbf{e}_kC \leftarrow C \cup \{\mathbf{y}\}
               end if
           end for
       end if
   end for
   return C
```

Note that this algorithm is *pleasantly parallel* since the description of vectors associated with indices  $\lambda \in \Lambda_N$  are independent from one another. The cost for producing each normal vector is  $O(N^2)$ , and no additional storage is needed.

# 8 The adjacency polytope homotopy for Kuramoto equations

We now return to the problem of finding all isolated complex solutions of (9) with the graph G being the

cycle graph  $C_N$ . Equivalently, these are the solutions of the unmixed synchronization equations  $F_{C_N}^R$  as defined in (10) (again with  $G = C_N$ ). Utilizing the unimodular regular triangulation of the adjacency polytope  $P_{C_N}$ , in this section, we describe a specialized *polyhedral homotopy* [25] construction for locating all of these complex solutions or the more general homotopy construction based on Khovanskii bases [4] *yet avoid the computationally expensive steps associated with polyhedral homotopy*.

Consider the function  $H_{C_N}: \mathbb{C}^n \times \mathbb{C} \to \mathbb{C}^n$  with  $H_{C_N}(\mathbf{x}, t) = (H_{C_N, 1}, \dots, H_{C_N, n})$  given by

$$H_{C_N,k} = c_k^R - \sum_{\{i,j\} \in \mathcal{E}(C_N)} \left( a_{ijk}^R \frac{x_i}{x_j} + a_{jik}^R \frac{x_j}{x_i} \right) t^{\omega_{ij}}$$

$$(17)$$

for  $k=1,\ldots,n$ , where  $\omega_{ij}=\omega(\mathbf{e}_i-\mathbf{e}_j)$  as given in (12) or (16) depending on the parity of N. Clearly,  $H_{C_N}(\mathbf{x},1)=F_{C_N}^R(\mathbf{x})$ . As t varies strictly between 0 and 1 within the interval [0,1],  $H_{C_N}(\mathbf{x},t)$  represents a smooth deformation of the unmixed synchronization system  $F_{C_N}^R$  (10). We shall show that under this deformation, the corresponding complex roots also vary smoothly. Thus, the deformation forms smooth paths reaching the complex roots of  $F_{C_N}^R$  and, equivalently, that of the algebraic synchronization system  $F_{C_N}$  (9).

**Proposition 13** For generic choices of the parameters, the solution set of  $H_{C_N}(\mathbf{x},t) = \mathbf{0}$  within  $\mathbb{C}^n \times (0,1)$  consists of  $N\binom{N-1}{\lfloor (N-1)/2 \rfloor}$  smooth curves that are smoothly parameterized by  $t \in (0,1)$ , and the limit points of these curves as  $t \to 1$  are precisely the isolated complex solutions of the unmixed synchronization system  $F_{C_N}^R(\mathbf{x}) = \mathbf{0}$  of (10).

This is a special version of the smoothness condition for the polyhedral homotopy, and its proof can be found in [25,30]. Here, we include a variation of the proof adapted from [30] for completeness, as the special choice of the lifting function prevents us from directly applying the general theorems which require generic liftings.

**Proof** As proved in [10], for generic choices of the parameters, the system  $H_{C_N}(\mathbf{x}, 1) \equiv F_{C_N}^R$  is in general position with respect to the adjacency polytope bound, i.e., it has the maximum number of isolated complex solutions.

Also note that for any  $t \neq 0$ ,  $H(\mathbf{x}, t)$  has the same form as (10) since the effect of t is only in scaling



the coefficients. We shall show that  $H(\mathbf{x}, t)$  remains a generic member of (9) for all  $t \in (0, 1]$  and hence all complex solutions of  $H(\mathbf{x}, t) = \mathbf{0}$  (as a system in  $\mathbf{x}$  only) are isolated and the total number matches the adjacency polytope bound  $N\binom{N-1}{\lfloor (N-1)/2 \rfloor}$ .

As noted in Remark 2, the genericity condition is characterized by an algebraic function D, the discriminant, which is a polynomial in the coefficients  $c_k^R$  and  $a_{ijk}^R t^{\omega_{ij}}$  for  $k=1,\ldots,n$  and  $\{i,j\} \in \mathcal{E}(C_N)$  such that  $F(\mathbf{x}) = H_{C_N}(\mathbf{x},t)$  is generic with respect to the adjacency polytope bound precisely when  $D \neq 0$ . Consider the univariate polynomial

$$g(t) = D((c_i^R)_{i=1}^n, (a_{ijk}^R t^{\omega_{ij}})_{\{i,j\} \in \mathcal{E}(C_N), k=1,\dots,n}).$$

By our genericity assumption,  $g(1) \neq 0$ , and therefore the polynomial g(t) is not the zero polynomial. It then has finitely many zeros within the unit disk of  $\mathbb{C}$ , say,  $r_1e^{\tau_1}, \ldots, r_\ell e^{\tau_\ell}$  for some  $\ell \in \mathbb{Z}^+$ . Picking a real value  $\tau \in [0, 2\pi]$  such that  $\tau \neq \tau_k$  for  $k = 1, \ldots, \ell$  will ensure  $g(e^{\tau}t) \neq 0$  for all  $t \in (0, 1)$ . But  $g(e^{\tau}t)$  describes the discriminant condition for the system  $H_{C_N,k}(\mathbf{x}, e^{\tau}t)$  given by

$$c_k^R - \sum_{\{i,j\} \in \mathcal{E}(C_N)} \left( a_{ijk}^R \frac{x_i}{x_j} + a_{jik}^R \frac{x_j}{x_i} \right) e^{\omega_{ij}\tau} t^{\omega_{ij}},$$

for k = 1, ..., n, which implies  $H_{C_N}(\mathbf{x}, e^{\tau}t)$  is in general position for all  $t \in (0, 1)$ .

Notice that the map  $\tau \mapsto e^{\omega_{ij}\tau}$  is finite-to-one, and the map  $a^R_{ijk} \mapsto a^R_{ijk} \cdot e^{\omega_{ij}\tau}$  is a nonsingular linear transformation on the coefficients  $\{a^R_{ijk}\}$ , which preserves genericity. We can conclude that for generic choices of the coefficients,  $H_{C_N}(\mathbf{x},t)$  will be in general position for  $t \in (0,1)$ .

This shows that at any fixed  $t \in (0, 1)$ , all solutions of  $H(\mathbf{x}, t) = \mathbf{0}$  in  $\mathbb{C}^n$  are isolated, and the total number is exactly the adjacency polytope bound  $N\binom{N-1}{\lfloor (N-1)/2\rfloor}$ . A direct application of the homotopy continuation theory is then sufficient to establish that the solution set of  $H(\mathbf{x}, t) = \mathbf{0}$  in  $\mathbb{C}^n \times (0, 1)$  forms paths that are smoothly parametrized by t. Furthermore, by continuity, the limit points of these paths as  $t \to 1$  must be all of the solutions of  $F_{C_N}^R(\mathbf{x}) = \mathbf{0}$  which is identical to that of  $F_{C_N}(\mathbf{x}) = \mathbf{0}$ .

The equation  $H_{C_N}(\mathbf{x}, t) = \mathbf{0}$  defines finitely many smooth paths in  $\mathbb{C}^n \times (0, 1)$  reaching all of the isolated complex solutions of the target synchronization system  $F_{C_N}(\mathbf{x}) = \mathbf{0}$ . The starting points of these paths at t = 0, however, cannot be determined directly since

 $H_{C_N}(\mathbf{x}, 0) = (c_1, \dots, c_n)$  which has no root in  $\mathbb{C}^n$ . This obstacle is surmounted via a technique similar to the main construction in polyhedral homotopy [25].

Recall that  $\Delta_N$  is the set of cells forming the unimodular triangulation of the adjacency polytope  $P_{C_N}$  (defined in (13) or (15) depending on the parity of N). For each cell  $T \in \Delta_N$ , we define the subset of (directed) edges

$$\mathcal{E}(T) = \{(i, j) \in \mathcal{E}(G) \mid \mathbf{e}_i - \mathbf{e}_j \in T\}.$$

Here, we do not assume the symmetry of edges, i.e.,  $(i, j) \in \mathcal{E}(T)$  does not imply  $(j, i) \in \mathcal{E}(T)$ . Define the *cell system*  $F_T = (F_{T,1}, \dots, F_{T,n})$  associated with the cell  $T \in \Delta_N$  to be

$$F_{T,k}(\mathbf{x}) = c_k^R - \sum_{(i,j) \in \mathcal{E}(T)} a_{ijk}^R \frac{x_i}{x_j}$$
(18)

for k = 1, ..., n. This system can be considered as a subsystem of the unmixed synchronization system (10) in the sense that it involves a subset of the terms in that system: only those terms corresponding to points in T. Indeed, T is exactly the Newton polytope of the corresponding cell system.

Remark 14 The cell systems defined here are refinements of the facet systems studied in [7]. Indeed, for odd N, they are exactly the facet systems since each  $T \in \Delta_N$  is the convex hull of a facet of the adjacency polytope  $P_{C_N}$  together with the origin. For even N values, however, the cell systems will be significant refinement of facet systems defined in [7]. Two particularly important advantages (18) offers are that it has a unique (complex) solution, and it can be solved easily and directly. This distinction will be explained in detail in Sect. 9.1.

Here, each cell  $T \in \Delta_N$  is a full-dimensional lattice simplex with normalized volume 1 (a primitive simplex). From classical results in toric algebraic geometry, we can deduce that the corresponding cell system has a unique solution.

**Lemma 15** For generic choices of complex constants  $\{c_i\}_{i=1}^n$  and  $\{a_{ij}, b_{ij}\}_{\{i,j\}\in\mathcal{E}(C_N)}$ , each cell system  $F_T(\mathbf{x})$ , as defined in (18), for  $T\in\Delta_N$  has a unique complex root, and this root is isolated and nonsingular.

A direct algebraic proof is also given in [7, Theorem 4], as the system  $F_T$  corresponds to a *primitive* subnetwork which has a unique generalized frequency



synchronization configuration. More importantly, as shown in that proof [7, Remark 5], after Gaussian elimination, such a system can be reduced to a special form of a binomial system which can be solved in linear time, i.e., in O(n) complex multiplications and divisions with no additional memory needed.

With this result, we modify the function (17) so that it defines a solution path that starts from the unique solution of the cell system  $F_T$ . This is essentially a specialized polyhedral homotopy [25] of the "unmixed" form using the triangulation found in the previous section.

**Definition 16** [Adjacency polytope homotopy] For each cell  $T \in \Delta_N$ , let  $(\alpha_1, \ldots, \alpha_n, 1) \in \mathbb{R}^{n+1}$  be the associated upward-pointing inner normal vector as given in Lemma 8 and Corollary 12. We define the *adjacency polytope homotopy* induced by this cell as the function  $H_T = (H_{T,1}, \ldots, H_{T,n}) : \mathbb{C}^n \times [0, 1] \to \mathbb{C}^n$  given by

$$H_{T,k}(\mathbf{y},t) = H_{C_N,k}(y_1 t^{\alpha_1}, \dots, y_n t^{\alpha_n}, t).$$
 (19)

Here,  $H_{C_N,k}$  is the function defined in (17). Recall that the collection of cells in  $\Delta_N$  form a regular triangulation of the adjacency polytope  $P_{C_N}$  which is also the Newton polytope of (10). By applying the construction of the unmixed form of polyhedral homotopy [25], we obtain the desired result: A homotopy that can locate all isolated complex solutions of the algebraic synchronization system  $F_{C_N}(\mathbf{x}) = \mathbf{0}$  as defined in (9).

**Theorem 17** For generic choices of the complex constants  $\{c_i\}_{i=1}^n$  and  $\{a_{ij}, b_{ij}\}_{\{i,j\} \in \mathcal{E}(C_N)}$ 

- 1. The solution set of  $H_T = \mathbf{0}$  within  $\mathbb{C}^n \times (0, 1)$  consists of a finite number of smooth paths parametrized by t, and the limit points of these paths as  $t \to 1$  are precisely the isolated solutions of  $F_{C_N}(\mathbf{x}) = \mathbf{0}$  in  $\mathbb{C}^n$ .
- 2. Among them, there is a unique path  $C_T(t)$  whose limit point  $C_T(0) = \lim_{t\to 0^+} C_T(t)$  is the unique solution of the cell system  $F_T(\mathbf{x}) = \mathbf{0}$  of (18).
- 3. The set of end points  $\{C_T(1) \mid T \in \Delta_N\}$  of paths induced by all cells is exactly the isolated  $\mathbb{C}$ -solution set of  $F_{C_N}(\mathbf{x}) = \mathbf{0}$ .

Remark 18 Here, the interpretation of "generic choices" still follows Remark 2: There is a nonzero polynomial D in  $\{c_i\}_{i=1}^n$  and  $\{a_{ij}, b_{ij}\}_{\{i,j\}\in\mathcal{E}_{C_N}}$  such that all choices of these coefficients at which D is nonzero are considered "generic." In particular, if these coefficients are

chosen at random, then, with probability one, the chosen coefficients will be generic. In other words, almost all choices are generic. Furthermore, it is sufficient to choose generic real constant terms  $\{c_i\}_{i=1}^n$  and symmetric coupling coefficients  $\{k_{ij}\}_{\{i,j\}\in\mathcal{E}_{C_N}}$ . That is, for almost all real constants  $\{c_i\}_{i=1}^n$  and  $\{k_{ij}\}_{\{i,j\}\in\mathcal{E}_{C_N}}$ , the conclusions of the above theorem still hold.

Remark 19 The theorem above assumes the coefficients to be generic. For special choices of the coefficients, e.g., in the special case of uniform coupling of  $k_{ij} = 1$ , this assumption will fail if N is divisible by 4, as detailed in [11].

The most practical way for handling such a nongeneric synchronization system  $F(\{c_i\}, \{k_{ij}\}; \boldsymbol{\theta})$  as in (3) is to consider a perturbed version  $F(\{c_i+\epsilon_i\}, \{k_{ij}+\epsilon_{ij}\}; \boldsymbol{\theta})$  with randomly chosen real numbers  $\epsilon_i$  and  $\epsilon_{ij}$  of sufficiently small magnitude. Then, with probability one, this perturbed synchronization system satisfies the assumption of the above theorem, and its synchronization configurations can be located by the adjacency polytope homotopy described here. The implicit function theorem ensures that regular solutions of the original synchronization system (solutions at which the Jacobian of the system is of full rank) can be approximated arbitrarily closely by the solutions of the perturbed system with sufficiently small values of  $\epsilon_i$  and  $\epsilon_{ij}$ .

Compared to a direct application of the polyhedral homotopy, the above construction has great computational advantages as summarized in Table 1.

Remark 20 From the viewpoint of numerical analysis, the stability of a homotopy formulation is a deep and complex problem that is outside the scope of this paper. Here, we only comment on one distinct advantage of the adjacency polytope homotopy over a direct application of the polyhedral homotopy method. In practical implementations of polyhedral homotopy, it is wellknown that the distribution of the exponents of the t parameter in the homotopy plays a crucial role in the numerical stability of the homotopy algorithm [19]. In particular, if the exponents of t spread over a wide range, the problem of tracking the homotopy paths can become extremely ill-conditioned and standard algorithms for path tracking become unstable. While many techniques have been developed to deal with this issue, it is much preferred if this problem can be avoided in the first place. In our construction, the exponents of t



Table 1 Computational advantages of the adjacency polytope homotopy

	Direct application ofpolyhedral homotopy	Adjacency polytopehomotopy
Construction of the homotopy	Requires the costly step of mixed cells computation	Each homotopy $H_T$ only requires one cell generated by Algorithm 1
Starting systems	Binomial systems which are usually solved in $O(n^3)$ time and additional memory	Special "primitive" system that can be solved in $O(n)$ time and requires no memory
Lifting function	Uses random image and requires numerical conditioning techniques	Uses values {0, 1, 2} and will not directly cause instability

in both (17) and Definition 16 involve small integers  $\{0, 1, 2\}$ , ensuring that the exponents of t in  $H_T(\mathbf{y}, t)$  consist of only small positive integers for relatively small N values.

#### 9 Interpretations

In this section, we interpret our main results in a wider context and draw connections to closely related problems. Even though the main result is an efficient homotopy method for locating complex synchronization configurations for the Kuramoto model on cycle networks, we shall show that our construction actually provides explicit solutions to other problems: the directed acyclic decomposition of cycle Kuramoto networks, and the self-intersection of a tropical hypersurface.

### 9.1 Directed acyclic decomposition of cycle networks

In recent work of the first author [7], a general scheme is proposed to decompose a Kuramoto network into smaller subnetworks supported by directed acyclic graphs while preserving certain properties of the synchronization configurations. This scheme utilizes the geometric properties of the adjacency polytope. Indeed, the subnetworks correspond to the facets of the adjacency polytope.

In this context, the constructions proposed in the present paper provide two important improvements to that decomposition scheme. First, the regular unimodular triangulation of the adjacency polytope  $P_{C_N}$  gives rise to a significant refinement for the directed acyclic

decomposition scheme which will decompose a cycle network into "primitive" subnetworks that can be analyzed easily and exactly. This was not possible for even *N* values with the original decomposition scheme. Second, as the starting system induced by the adjacency polytope homotopy (17) can be solved easily and efficiently. Finally, since the explicit formula for the generic root count is known (Sect. 5), the number of solution paths induced by the homotopy proposed in Sect. 8 matches the generic root count exactly, and thus will not produce extraneous solution paths in the generic situation. This feature was not established for the original decomposition scheme and the associated homotopy method.

To see how the regular unimodular triangulation described in Sect. 6 gives rises to a decomposition of the Kuramoto network, we first define the subnetwork corresponding to a cell.

**Definition 21** Let  $\Delta_N$  be the regular subdivision of  $P_{C_N}$  defined in (13) and (15). For each cell  $T \in \Delta_N$ , we define the *directed acyclic subnetwork* associated with T to be the graph  $(\{0, \ldots, N-1\}, \mathcal{E}(T))$  where

$$\mathcal{E}(T) = \{(i, j) \in \mathcal{E}(C_N) \mid \mathbf{e}_i - \mathbf{e}_j \in T\}.$$

This is a refinement of the definition in [7] where subnetworks correspond to facets of the adjacency polytope. In contrast, subnetworks defined above come from a triangulation which, in the case of even N values, are associated with simplices in the facets of  $P_{C_N}$ .

As established in [7], such a subnetwork associated with a cell is always an *acyclic* graph, which justifies its name (directed acyclic subnetwork). Moreover, such subnetworks are of the simplest possible form known as "primitive" subnetworks.



**Definition 22** [Primitive subnetwork [7]] A subnetwork associated with a cell is said to be *primitive* if it contains exactly n = N - 1 directed edges.

Primitive subnetworks are the smallest directed acyclic subnetworks that are weakly connected and contain all oscillators. More importantly, their (generalized) synchronization configurations can be analyzed easily and exactly. Note that since each cell  $T \in \Delta_N$  is a simplex of dimension n containing exactly n nonzero points of the form  $\mathbf{e}_i - \mathbf{e}_j$  for  $i \neq j$ , we can see that the induced subnetwork must be primitive.

**Proposition 23** Let  $\Delta_N$  be the regular unimodular triangulation of  $P_{C_N}$ . For each cell  $T \in \Delta_N$ , the associated directed acyclic subnetwork is primitive.

In other words, under the assumption of generic coefficients, each primitive subnetwork corresponds to a complex solution of the algebraic synchronization system (9) through the adjacency polytope homotopy

(Definition 16). Figure 3 shows the directed acyclic subnetworks of a cycle network with 4 nodes induced by the triangulation  $\Delta_N$ . All subnetworks are primitive. In contrast, the decomposition scheme studied in previous work [7], shown in Fig. 4, produces subnetworks that are not primitive.

#### 9.2 A tropical interpretation

Even though it was not stated explicitly, the procedure that resulted in the adjacency polytope homotopy (17) is actually rooted from tropical algebraic geometry [32]. In this section, we provide the interpretation from the tropical viewpoint.

Recall that we started with the unmixed form of the algebraic synchronization equations (10). If we consider the valuation on the field of coefficients given by

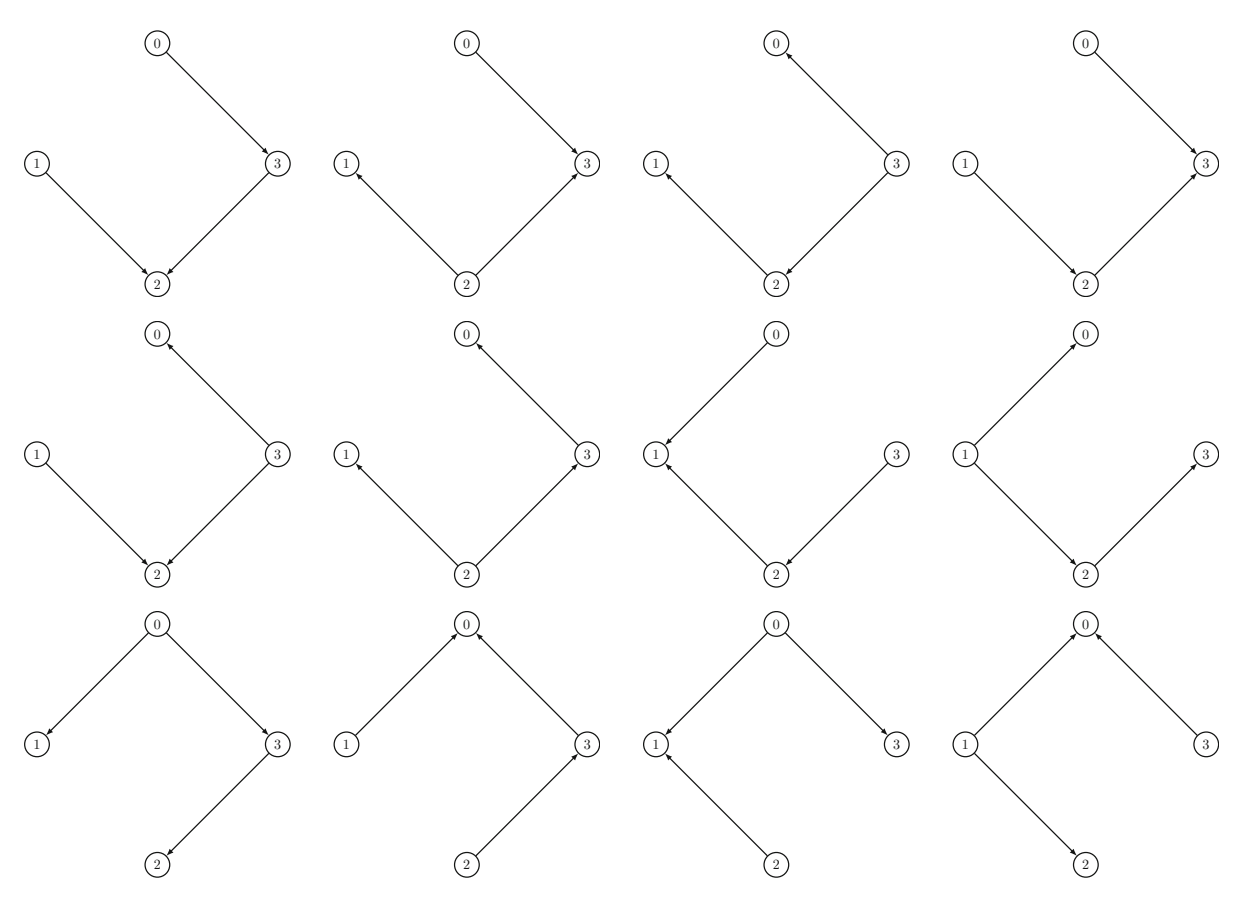
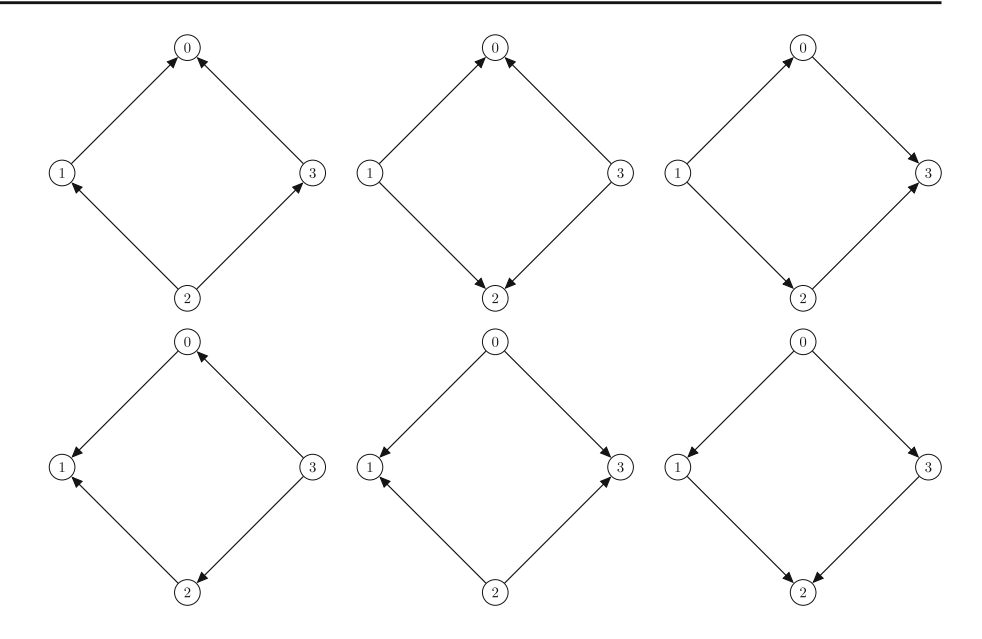


**Fig. 3** Directed acyclic subnetworks of a cycle network with 4 nodes induced by the refined decomposition scheme developed in this paper. Every subnetwork is *primitive*. This is to be compared with the original coarser decomposition scheme shown in Fig. 4



Fig. 4 Directed acyclic subnetworks of a cycle network with 4 nodes induced by the coarser decomposition scheme originally proposed in [7]. None of the subnetworks are primitive



$$val(c_i^R) = 0 \quad and \tag{20}$$

$$val(a_{ijk}^R) = \begin{cases} 2 & \text{if N is even and } (i, j) = (1, 0) \\ 1 & \text{otherwise,} \end{cases}$$
 (21)

which mirrors the choices of the weights given in (12) and (16), then the tropicalizations of the n polynomials in (1) are identical and they define a common tropical hypersurface. The main results developed in Sect. 6 can thus be interpreted tropically: The valuation defined above induces the simplest (stable) self-intersection.

**Proposition 24** Let  $h = \operatorname{trop}(F_{C_N,k}^R)$  for  $k = 1, \ldots, n$  be the tropicalization of (10) with respect to the valuation given in (20). Then, the tropical hypersurface defined by h has exactly  $N\binom{N-1}{\lfloor (N-1)/2 \rfloor}$  self-intersection points, and each intersection is of multiplicity one.

As discussed in Remark 10, the special choice of the valuation (20) is an important condition for this result to hold. Using only 0-1 valuations, for example, will not produce self-intersections with multiplicity one. One of the key contributions of this paper is the explicit formula for these self-intersection points. These tropical self-intersection points are precisely the tropicalizations of the curves defined by (17).

### 10 An example

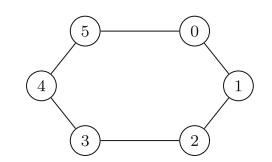
In this section, we illustrate the workflow of the proposed algorithm through the example of a cycle network consisting of 6 oscillators as shown in Fig. 5. This example will assume natural frequencies  $c_1 = 0.011$ ,  $c_2 = 0.012$ ,  $c_3 = 0.013$ ,  $c_4 = 0.014$ , and  $c_5 = 0.015$  (relative to a rotating frame of reference determined by the mean natural frequencies) and coupling coefficients  $k_{ij} = 1$ . The edge set of the underlying graph  $C_6$  is

$$\{\{0, 1\}, \{1, 2\}, \{2, 3\}, \{3, 4\}, \{4, 5\}, \{5, 0\}\},\$$

and the adjacency polytope is a full-dimensional polytope in  $\mathbb{R}^5$  given by the convex hull of the points

as well as the origin. Algorithm 1 produces 60 cells that form a unimodular triangulation of the adjacency polytope; the implementation is described in "Code availability" section. Since all of the cells will be handled in the same process and are unimodularly equivalent to one another, in this example, we will focus on a single cell.

**Fig. 5** A cycle network of six oscillators





One of the cells produced by Algorithm 1 is the full-dimensional simplex in  $\mathbb{R}^5$  spanned by the subset

$$E = \left\{ \begin{bmatrix} -1\\1\\0\\0\\0\\0 \end{bmatrix}, \begin{bmatrix} 0\\-1\\1\\0\\0\\0 \end{bmatrix}, \begin{bmatrix} 0\\0\\0\\1\\-1\\0 \end{bmatrix}, \begin{bmatrix} 0\\0\\0\\0\\1\\0 \end{bmatrix}, \begin{bmatrix} 0\\0\\0\\0\\0\\0\\0 \end{bmatrix}, \begin{bmatrix} 0\\0\\0\\0\\0\\0\\0 \end{bmatrix}, \right\}.$$

It corresponds to the primitive subnetwork shown in Fig. 6 and the upward pointing inner normal vector

$$\hat{\boldsymbol{\alpha}} = \begin{bmatrix} \alpha_1 \\ \alpha_2 \\ \alpha_3 \\ \alpha_4 \\ \alpha_5 \\ 1 \end{bmatrix} = \begin{bmatrix} -1 \\ -2 \\ -3 \\ -2 \\ -1 \\ 1 \end{bmatrix}.$$

The adjacency polytope homotopy (Definition 16) induced by this cell  $H_T = (H_{T,1}, \dots, H_{T,5})$  is given by

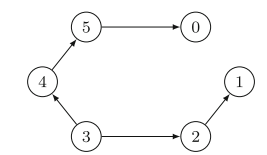
$$H_{T,k}(\mathbf{y},t) = c_k^R - \sum_{\{i,j\} \in E} \left( a_{ijk}^R \frac{y_i t^{\alpha_i}}{y_j t^{\alpha_j}} + a_{jik}^R \frac{y_j t^{\alpha_j}}{y_i t^{\alpha_i}} \right) t^{\omega_{ij}}.$$

At t = 0,  $H_T$  reduces to the cell system (defined in (18))  $F_T = (F_{T,1}, \ldots, F_{T,5})$  associated with this cell, which given by

$$c_k^R - a_{21k}^R \frac{x_2}{x_1} - a_{32k}^R \frac{x_3}{x_2} - a_{34k}^R \frac{x_3}{x_4} - a_{45k}^R \frac{x_4}{x_5} - a_{50k}^R \frac{x_5}{x_0}$$

for k = 1, 2, 3, 4, 5. This cell system has a unique complex solution, and it can be computed directly and efficiently [7, Remark 5]. Using it as the starting point, we can trace the solution path defined by  $H_T(\mathbf{y}, t) = \mathbf{0}$  from t = 0 to t = 1 via path trackers described in "Code availability" section, and we obtain an approximation of the complex solution given by

**Fig. 6** A primitive subnetwork corresponds to a cell



$$x_1 = 9.999636994703 \cdot 10^{-1} - 8.520548236360 \cdot 10^{-3}$$
**i**  
 $x_2 = 9.996068365590 \cdot 10^{-1} - 2.803876432684 \cdot 10^{-2}$ **i**  
 $x_3 = 9.982263386348 \cdot 10^{-1} - 5.953298749315 \cdot 10^{-2}$ **i**  
 $x_4 = -9.998870074708 \cdot 10^{-1} + 1.503237480704 \cdot 10^{-2}$ **i**  
 $x_5 = -9.972937024033 \cdot 10^{-1} + 7.352054824607 \cdot 10^{-2}$ **i**. They correspond to the complex phase angles

$$\theta_1 = -8.520651337993 \cdot 10^{-3} - 2.882462982872 \cdot 10^{-13} \mathbf{i}$$

$$\theta_2 = -2.804243951050 \cdot 10^{-2} - 2.336632165329 \cdot 10^{-13} \mathbf{i}$$

$$\theta_2 = -5.956820960829 \cdot 10^{-2} + 1.279509845221 \cdot 10^{-10} \mathbf{i}$$

$$\theta_2 = 3.126559712575 \cdot 10^0 - 6.254418586421 \mathbf{i} 0^{-13} \mathbf{i}$$

$$\theta_2 = 3.068005710633 \cdot 10^0 + 6.615774118443 \cdot 10^{-11} \mathbf{i},$$

which produce a good approximation of a real synchronization configuration. Here, we only show the approximation directly obtained from a numerical homotopy continuation implementation using double precision floating point arithmetic before a "refinement" procedure is applied. In typical applications, local solvers such as Newton's iterations should be applied to this approximation and refine the numerical solution to any desired accuracy.

The same process can be repeated for all 60 cells, and all 60 complex solutions can be computed efficiently. Indeed, all 60 complex solutions obtained are close approximations of real synchronization configurations. Since the homotopy paths are independent from one another, the computation of the 60 solutions can be carried out in parallel.

#### 11 Conclusions

Following the volume computation result in [10], this paper aims to deepen the geometric understanding of adjacency polytopes associated with a cycle Kuramoto network and use this information to explore three aspects of Kuramoto equations:

- 1. To create an efficient polyhedral-like homotopy for solving Kuramoto equations;
- To explicitly describe directed acyclic decompositions of Kuramoto networks into *primitive* subnetworks;
- 3. To understand the stable intersections of the tropical hypersurfaces defined by Kuramoto equations.

First, we derived the explicit formula for a regular unimodular triangulation of the adjacency polytope



 $P_{C_N}$  associated with a cycle graph of N nodes for any N > 2. This greatly strengthens the results from [10] where only the normalized volume of  $P_{C_N}$  is known.

Then, using this regular unimodular triangulation, we develop a homotopy continuation algorithm based on the well-established polyhedral homotopy method yet has the distinct advantage that it entirely sidesteps the costly mixed volume/cells computation step. This homotopy is also a significant improvement over the directed acyclic homotopy proposed in [7] since it deforms the Kuramoto system into simplest possible subsystems each having a unique solution. From the computational viewpoint, the proposed homotopy also offers important advantages in numerical conditions, efficiency, and scalability as discussed in Remark 20.

The third contribution of this paper is a significantly refined version of the directed acyclic decomposition scheme originally proposed in [7]. The regular unimodular triangulation proposed here induces a decomposition of a cycle Kuramoto network into the smallest possible components known as primitive subnetworks. Primitive subnetworks are of great value since they each have a unique complex synchronization configuration which can be computed easily and efficiently. This is to be compared with the situation of the original decomposition scheme where the resulting subnetworks, in general, may not be primitive.

Finally, interpreted in the context of tropical geometry, our result provides explicit formula for all stable intersections of the tropical hypersurfaces defined by the unmixed form of the Kuramoto system under a special choice of the valuation. The induced tropical intersections are particularly nice as we have shown that every intersection point is of multiplicity 1.

**Funding** This work was funded, in part, by the AMS Simons Travel Grant, Auburn University at Montgomery Research Grant-in-Aid Program, and the NSF under award numbers DMS-1923099 and DMS-1922998.

Code availability The main algorithms for generating the cells in the regular unimodular triangulation  $\Delta_N$  of  $P_{C_N}$  are implemented in an open source Python package kap-cycle [6]. In addition to the cells, this package also produces the upward-pointing inner normals corresponding to each cell. That is, it provides all the necessary information for bootstrapping the adjacency polytope homotopy proposed in Sect. 8. The actual tracking of the homotopy paths can be done via a variety of robust numerical software packages known as "path trackers." The cal-

culations involved in the example described in Sect. 10 are carried out by the GPU-accelerated path tracker libdh [9].

#### **Declarations**

Conflict of interest Not applicable.

#### References

- Ardila, F., Beck, M., Hoşten, S., Pfeifle, J., Seashore, K.: Root polytopes and growth series of root lattices. SIAM J. Discrete Math. 25(1), 360–378 (2011). https://doi.org/10. 1137/090749293
- Baillieul, J., Byrnes, C.: Geometric critical point analysis of lossless power system models. IEEE Trans. Circuits Syst. 29(11), 724–737 (1982). https://doi.org/10.1109/TCS. 1982.1085093
- Balestra, C., Kaiser, F., Manik, D., Witthaut, D.: Multistability in lossy power grids and oscillator networks. Chaos Interdiscip. J. Nonlinear Sci. 29, 123119 (2019). https://doi. org/10.1063/1.5122739
- Burr, M., Sottile, F., Walker, E.: Numerical homotopies from Khovanskii bases (2020). https://github.com/EliseAWalker/ KhovanskiiHomotopy/
- Casetti, L., Pettini, M., Cohen, E.G.D.: Phase transitions and topology changes in configuration space. J. Stat. Phys. 111, 1091–1123 (2003)
- Chen, T.: chentianran/kap-cycle: Version 1.0.1 (2018). https://doi.org/10.5281/zenodo.1439501
- Chen, T.: Directed acyclic decomposition of Kuramoto equations. Chaos Interdiscip. J. Nonlinear Sci. 29(9), 093101 (2019). https://doi.org/10.1063/1.5097826
- Chen, T.: Unmixing the mixed volume computation. Discrete Comput. Geom. (2019). https://doi.org/10.1007/ s00454-019-00078-x
- Chen, T.: Gpu-accelerated path tracker for polyhedral homotopy (2021). arXiv:2111.14317v1
- Chen, T., Davis, R., Mehta, D.: Counting equilibria of the Kuramoto model using birationally invariant intersection index. SIAM J. Appl. Algebra Geom. 2(4), 489–507 (2018). https://doi.org/10.1137/17M1145665
- Chen, T., Korchevskaia, E.: On the root count of algebraic Kuramoto equations in cycle networks with uniform coupling (2019). arXiv:1912.06241
- Chen, T., Marecek, J., Mehta, D., Niemerg, M.: Three formulations of the Kuramoto model as a system of polynomial equations. In: 2019 57th Annual Allerton Conference on Communication, Control, and Computing, Allerton 2019, pp. 810–815. Institute of Electrical and Electronics Engineers Inc. (2019). https://doi.org/10.1109/ALLERTON.2019.8919934
- De Loera, J.A., Rambau, J., Santos, F.: Triangulations. In: Algorithms and Computation in Mathematics, vol. 25. Springer, Berlin (2010). https://doi.org/10.1007/978-3-642-12971-1. Structures for algorithms and applications
- Delabays, R., Coletta, T., Jacquod, P.: Multistability of phase-locking and topological winding numbers in locally



- coupled Kuramoto models on single-loop networks. J. Math. Phys. **57**(3), 032701 (2016)
- Delabays, R., Coletta, T., Jacquod, P.: Multistability of phase-locking in equal-frequency Kuramoto models on planar graphs. J. Math. Phys. 58(3), 032703 (2017)
- Delucchi, E., Hoessly, L.: Fundamental polytopes of metric trees via parallel connections of matroids (2016)
- Dörfler, F., Bullo, F.: Synchronization in complex networks of phase oscillators: a survey. Automatica 50(6), 1539–1564 (2014). https://doi.org/10.1016/j.automatica.2014.04.012
- Fulton, W.: Introduction to Toric Varieties, vol. 131. Princeton University Press, Princeton (1993)
- Gao, T., Li, T.Y., Verschelde, J., Wu, M.: Balancing the lifting values to improve the numerical stability of polyhedral homotopy continuation methods. Appl. Math. Comput. 114(2–3), 233–247 (2000). https://doi.org/10.1016/ S0096-3003(99)00115-0
- Grayson, D.R., Stillman, M.E.: Macaulay2, a software system for research in algebraic geometry. http://www.math.uiuc.edu/Macaulay2/
- Hellmann, F., Schultz, P., Jaros, P., Levchenko, R., Kapitaniak, T., Kurths, J., Maistrenko, Y.: Network-induced multistability through lossy coupling and exotic solitary states.
   Nat. Commun. 2020(11), 1–9 (2020). https://doi.org/10.1038/s41467-020-14417-7
- Higashitani, A., Jochemko, K., Michałek, M.: Arithmetic aspects of symmetric edge polytopes. Mathematika 65(3), 763–784 (2019). https://doi.org/10.1112/s0025579319000147
- Higashitani, A., Kummer, M., Michałek, M.: Interlacing Ehrhart Polynomials of Reflexive Polytopes (2016). https:// doi.org/10.1007/s00029-017-0350-6
- Higashitani, A., Kummer, M., Michałek, M.: Interlacing Ehrhart polynomials of reflexive polytopes. Sel. Math. (N.S.) 23(4), 2977–2998 (2017). https://doi.org/10.1007/ s00029-017-0350-6
- Huber, B., Sturmfels, B.: A polyhedral method for solving sparse polynomial systems. Math. Comput. 64(212), 1541–1555 (1995). https://doi.org/10.1090/ S0025-5718-1995-1297471-4
- Kastner, M.: Stationary-point approach to the phase transition of the classical XY chain with power-law interactions. Phys. Rev. E 83(3), 031114 (2011)
- Kaveh, K., Khovanskii, A.: Newton-Okounkov bodies, semigroups of integral points, graded algebras and intersection theory. Ann. Math. 176(2), 925–978 (2012). https:// doi.org/10.4007/annals.2012.176.2.5
- Kaveh, K., Khovanskii, A.G.: Mixed volume and an extension of theory of divisors. Mosc. Math. J. 10(2), 343–375 (2010)
- Kuramoto, Y.: Self-Entrainment of a Population of Coupled Non-linear Oscillators. Lecture Notes in Physics, pp. 420– 422. Springer, Berlin (1975)
- Li, T.Y.: Numerical Solution of Polynomial Systems by Homotopy Continuation. In: P.G. Ciarlet (ed.) Handbook of Numerical Analysis: Special Volume: Foundations of Computational Mathematics, vol. 11, p. 470. North-Holland (2003). https://doi.org/10.1016/S1570-8659(02)11004-0
- 31. Lindberg, J., Zachariah, A., Boston, N., Lesieutre, B.C.: The distribution of the number of real solutions to the power flow equations

- Maclagan, D., Sturmfels, B.: Introduction to Tropical Geometry. Graduate Studies in Mathematics. American Mathematical Society, Providence (2015)
- Manik, D., Timme, M., Witthaut, D.: Cycle flows and multistability in oscillatory networks. Chaos 27(8), 083123 (2017). https://doi.org/10.1063/1.4994177
- Matsui, T., Higashitani, A., Nagazawa, Y., Ohsugi, H., Hibi,
   T.: Roots of Ehrhart polynomials arising from graphs. J.
   Algebraic Combin. 34(4), 721–749 (2011). https://doi.org/ 10.1007/s10801-011-0290-8
- Mehta, D., Daleo, N.S., Dörfler, F., Hauenstein, J.D.: Algebraic geometrization of the Kuramoto model: equilibria and stability analysis. Chaos Interdiscip. J. Nonlinear Sci. 25(5), 053103 (2015). https://doi.org/10.1063/1.4919696
- Muller, L., Mináč, J., Nguyen, T.T.: Algebraic approach to the Kuramoto model. Phys. Rev. E 104, L022201, 093101 (2021). https://doi.org/10.1103/PHYSREVE.104. L022201/FIGURES/4/MEDIUM
- Nill, B.: Classification of pseudo-symmetric simplicial reflexive polytopes. In: Algebraic and Geometric Combinatorics, Contemp. Math., vol. 423, pp. 269–282. Amer. Math. Soc., Providence (2006). https://doi.org/10.1090/ conm/423/08082
- Ochab, J., Gora, P.: Synchronization of coupled oscillators in a local one-dimensional Kuramoto model. Acta Phys. Pol. Ser. B Proc. Suppl. 3(2), 453–462 (2010)
- Ohsugi, H., Hibi, T.: Centrally symmetric configurations of integer matrices. Nagoya Math. J. 216, 153–170 (2014). https://doi.org/10.1215/00277630-2857555
- Ohsugi, H., Shibata, K.: Smooth Fano polytopes whose Ehrhart polynomial has a root with large real part. Discrete Comput. Geom. 47(3), 624–628 (2012). https://doi.org/10. 1007/s00454-012-9395-7
- Postnikov, A.: Permutohedra, associahedra, and beyond. Int. Math. Res. Not. IMRN 6, 1026–1106 (2009). https://doi.org/ 10.1093/imrn/rnn153
- Sommese, A.J., Wampler, C.W.: The Numerical Solution of Systems of Polynomials Arising in Engineering and Science. World Scientific, Singapore (2005). https://doi.org/10.1142/ 5763
- Xi, K., Dubbeldam, J.L., Lin, H.X.: Synchronization of cyclic power grids: equilibria and stability of the synchronous state. Chaos Interdiscip. J. Nonlinear Sci. 27(1), 013109 (2017)
- 44. Xin, X., Kikkawa, T., Liu, Y.: Analytical solutions of equilibrium points of the standard kuramoto model: 3 and 4 oscillators. In: American Control Conference (ACC), 2016, pp. 2447–2452. IEEE (2016)

**Publisher's Note** Springer Nature remains neutral with regard to jurisdictional claims in published maps and institutional affiliations.

